Application of Hermitian time-dependent coupled-cluster response *Ansätze* of second order to excitation energies and frequency-dependent dipole polarizabilities

Gero Wälz,[1] Daniel Kats,[2] Denis Usvyat,[1] Tatiana Korona,[3] and Martin Schütz[1]

[1]*Institute of Physical and Theoretical Chemistry, University of Regensburg, Universitätsstraße 31, D-93040 Regensburg, Germany*

[2]*Center for Computational Chemistry, School of Chemistry, University of Bristol, Bristol BS8 1TS, United Kingdom*

[3]*Faculty of Chemistry, University of Warsaw, ul. Pasteura 1, PL-02-093 Warsaw, Poland*

(Received 1 October 2012; published 29 November 2012)

Linear-response methods, based on the time-dependent variational coupled-cluster or the unitary coupled-cluster model, and truncated at the second order according to the Møller-Plesset partitioning, i.e., the TD-VCC[2] and TD-UCC[2] linear-response methods, are presented and compared. For both of these methods a Hermitian eigenvalue problem has to be solved to obtain excitation energies and state eigenvectors. The excitation energies thus are guaranteed always to be real valued, and the eigenvectors are mutually orthogonal, in contrast to response theories based on "traditional" coupled-cluster models. It turned out that the TD-UCC[2] working equations for excitation energies and polarizabilities are equivalent to those of the second-order algebraic diagrammatic construction scheme ADC(2). Numerical tests are carried out by calculating TD-VCC[2] and TD-UCC[2] excitation energies and frequency-dependent dipole polarizabilities for several test systems and by comparing them to the corresponding values obtained from other second- and higher-order methods. It turns out that the TD-VCC[2] polarizabilities in the frequency regions away from the poles are of a similar accuracy as for other second-order methods, as expected from the perturbative analysis of the TD-VCC[2] polarizability expression. On the other hand, the TD-VCC[2] excitation energies are systematically too low relative to other second-order methods (including TD-UCC[2]). On the basis of these results and an analysis presented in this work, we conjecture that the perturbative expansion of the Jacobian converges more slowly for the TD-VCC formalism than for TD-UCC or for response theories based on traditional coupled-cluster models.

DOI: 10.1103/PhysRevA.86.052519 PACS number(s): 31.15.bw, 31.15.ag

I. INTRODUCTION

Coupled-cluster (CC) theory [1] is one of the most successful computational methods for calculating dynamic electron correlation in molecules. The exponential *Ansatz* for the CC wave function $|\Psi\rangle = \exp(\mathbf{T})|0\rangle$ ensures size extensivity of the method also for truncated cluster operators $\mathbf{T}$ by including the required disconnected clusters. Furthermore, a CC wave function, even based on a cluster operator truncated, e.g., beyond doubles substitutions (CCSD), contains all possible excited determinants of the corresponding full configuration interaction (CI) *Ansatz*; the coefficients of the higher, i.e., beyond doubles, substitutions though are approximated by corresponding products of singles and doubles amplitudes. From that angle the CC *Ansatz* can also be considered as a method leading to an appropriate tensor decomposition of the full CI coefficients related to higher excited determinants. For a comprehensive review of coupled-cluster theory, we refer to Ref. [2].

Since the variational determination of the CC amplitudes is too difficult, the *projected Schrödinger equation* formalism (sometimes called "traditional" CC theory [3]) is commonly employed. Here, the CC wave function is inserted into the Schrödinger equation, which in turn is projected against the reference (yielding the energy), and against the determinants covered by the cluster operator $\mathbf{T}$ (yielding the amplitude equations, i.e., as many equations as there are amplitudes to be determined). Usually, prior to projection the Schrödinger equation is multiplied by $\exp(-\mathbf{T})$. This delivers the so-called "linked" CC equations, which are size extensive term by term and terminate after the fourth power of $\mathbf{T}$ regardless of the number of electrons and the truncation in $\mathbf{T}$.

CC methods based on canonical molecular orbitals (MOs) exhibit a rather steep polynomial scaling of the computational cost with system size $\mathcal{N}$, e.g., $O(\mathcal{N}^6)$ and $O(\mathcal{N}^7)$ for CCSD and CCSD(T), respectively, where the latter (CCSD with a perturbative triples correction) [4] represents the "gold standard" in quantum chemistry. Polynomial scaling of the computational cost is already a great achievement compared to the factorially hard problem of full CI, but still limits the application of CC theory to systems of small or medium size. Low- (even linear) scaling CC methods can be devised by substituting the canonical by local MOs and exploiting the short-range nature of dynamic correlation effects [5–10].

Properties and electronically excited states are, in the framework of "traditional" CC theory, accessible through time-dependent (TD) response [11–14], or equation-of-motion (EOM) formalisms [15–17]. Pioneering work on this topic has been published already in the late 1970s [18–20]. TD response and EOM-CC approaches differ significantly in their perspective of electronically excited states. EOM-CC considers excited states as the eigenstates of the (time-independent) similarity-transformed coupled-cluster Hamiltonian $\hat{\mathbf{H}} = \exp(-\mathbf{T})\mathbf{H}\exp(\mathbf{T})$ in the basis of singly, doubly, etc., excited configurations. It is therefore a (truncated) configuration interaction method employing the $\hat{\mathbf{H}}$ Hamiltonian and the correlated CC wave function as the reference. The TD response method, on the other hand, considers the excitation energies as time- or frequency-dependent ground-state properties, i.e., as the poles of the dynamic polarizability. The TD response thus provides a very general framework, which can be used in the context of density functional, Hartree-Fock, or CC theory. Interestingly,

despite the different vantage point, both methods lead, for a traditional CC theory like CCSD, to analogous equations determining the excitation energies, although transition strengths and other properties of excited states differ. In the present work we focus on the TD response formalism.

Traditional CC theory has a disadvantage that it lacks Hermiticity: Since $\exp(\mathbf{T})$ contains exclusively excitation operators, the CC similarity-transformed Hamiltonian $\hat{\mathbf{H}}$ is not Hermitian. The absence of deexcitation operators directly implies the practical gains mentioned above, but also has undesirable consequences, particularly so for excited states. Specifically, the eigenvectors of the nonsymmetric Jacobian representing the excited states are nonorthogonal, and the excitation energies may become complex [21,22], especially for distorted geometries and close to conical intersections. It is therefore attractive to investigate alternative variational CC formalisms, and to develop time-dependent response theories on top of those. Quite a few papers devoted to alternative CC theories have been published so far; these refer mainly to the ground-state energy [23–33], but there are also some contributions addressing molecular ground-state properties [34–39].

Recently, some of us presented a time-dependent response approach on the basis of variational CC theory (cf. Ref. [40], denoted as Paper I in the following), which is targeting excitation energies and first-order properties of excited states. The problem with the nonterminating series of diagrams, which is due to the presence of deexcitation operators $\mathbf{T}^\dagger$, was solved in a pragmatic way by utilizing a Møller-Plesset (MP) perturbation expansion and omitting terms which contribute at an order higher than some selected power n of the fluctuation operator $\mathbf{W}$ to the time-dependent quasienergy ($\mathbf{W} = \mathbf{H} - \mathbf{F}$, where $\mathbf{H}$ is the Hamiltonian and $\mathbf{F}$ is the Fock operator). Within this framework a hierarchy of methods of increasing accuracy can be derived. The different levels of this hierarchy were denoted by the acronym TD-VCC[n] (time-dependent variational coupled cluster), where n stands for the largest fully included order of $\mathbf{W}$. The first two orders $n = 0$ and $n = 1$ are equivalent to the Koopmans-like treatment (orbital energy differences) and the configuration interaction singles (CIS) method for excitation energies, respectively. The lowest correlated level appears at second order and is therefore denoted as TD-VCC[2].

In the present contribution we explore, in the same spirit, yet another time-dependent response approach (denoted by the acronym TD-UCC[n]), which is based on the unitary coupled-cluster (UCC) formalism [26,27], rather than VCC. Moreover, we present numerical excitation energies and dynamic dipole polarizabilities for both of these methods, and compare these to other relevant approaches, such as TD-CC2 [41], TD-CCSD [42,43] (equivalent to EOM-CCSD for excitation energies [16], but not for polarizabilities [44,45]), TD-CC3 [46], and other alternative CC theories for properties [30,36,47].

II. THEORY

A. Linear response

In this section an "in a nutshell" review of linear-response theory is given, in order to prepare the ground for the subsequent discussion. For a detailed discussion of response theory, based on the time-averaged quasienergy, we refer to Ref. [14], and references therein.

The time-independent Hamiltonian $\mathbf{H}^{(0)}$ is augmented by a general time-dependent perturbation operator, i.e.,

$$\mathbf{H}(t) = \mathbf{H}^{(0)} + \mathbf{V}(t), \quad \text{with} \quad \mathbf{V}(t) = \sum_{k=-N}^{N} \exp(-i\omega_k t)\mathbf{V}^{\omega_k} \quad \text{and} \quad \mathbf{V}^{\omega_k} = \sum_X \epsilon_X(\omega_k)\mathbf{X}. \tag{1}$$

For simplicity, the k-index summation can be restricted to only two terms by setting $N = 1$. This restriction does not affect results of linear-response theory, but only of higher orders. The time evolution of the wave function $|\tilde{\Psi}(t)\rangle$, written in the phase-isolated form as

$$|\bar{\Psi}(t)\rangle = e^{iF(t)}|\tilde{\Psi}(t)\rangle, \tag{2}$$

is governed by the time-dependent Schrödinger equation

$$\mathbf{H}(t)|\bar{\Psi}(t)\rangle = i\frac{\partial}{\partial t}|\bar{\Psi}(t)\rangle. \tag{3}$$

Note that the (still time-dependent) wave function $|\tilde{\Psi}(t)\rangle$ is restricted such that it becomes equivalent to the time-independent solution $|\Psi\rangle$ (with $\mathbf{H}^{(0)}|\Psi\rangle = E|\Psi\rangle$) for vanishing perturbation $\mathbf{V}(t)$. Inserting Eq. (2) in Eq. (3) and projecting onto $\langle\tilde{\Psi}(t)|$ straightforwardly yields the quasienergy as the time derivative of the phase of $|\bar{\Psi}(t)\rangle$, i.e.,

$$Q(t) = \dot{F}(t) = \langle\tilde{\Psi}(t)|\bar{\mathbf{H}}(t)|\tilde{\Psi}(t)\rangle, \quad \text{with} \quad \bar{\mathbf{H}}(t) = \mathbf{H}(t) - i\frac{\partial}{\partial t}. \tag{4}$$

$Q(t)$ is the formal time-dependent analog of the energy [to which it reduces for vanishing $\mathbf{V}(t)$], and of central importance for the time-dependent formalism. The derivative of the *time-averaged* (over the period T) quasienergy with respect to the perturbation strength $\epsilon_X(\omega_X)$ is equivalent to the time-averaged expectation value over an operator $\mathbf{X}$,

$$\begin{aligned}\frac{d\{Q(t)\}_T}{d\epsilon_X(\omega_X)} &= \{\langle\tilde{\Psi}(t)|\mathbf{X}|\tilde{\Psi}(t)\rangle\}_T \\ &= \frac{1}{T}\int_{-T/2}^{T/2} dt\,\langle X\rangle_0 e^{-i\omega_X t} + \sum_{k_1} e^{-i(\omega_X+\omega_{k_1})t} \\ &\quad\times \sum_Y \epsilon_Y(\omega_{k_1})\langle\langle X;Y\rangle\rangle_{\omega_X\omega_{k_1}} + \cdots \\ &= \langle X\rangle_0\delta(\omega_X) + \sum_{k_1}\sum_Y \epsilon_Y(\omega_{k_1})\langle\langle X;Y\rangle\rangle_{\omega_X\omega_{k_1}} \\ &\quad\times \delta(\omega_X+\omega_{k_1}) + \cdots;\end{aligned} \tag{5}$$

hence there is the direct equality

$$\frac{d^2\{Q^{(2)}(t)\}_T}{d\epsilon_X(\omega_X)d\epsilon_Y(\omega_Y)} \equiv \langle\langle X;Y\rangle\rangle_{\omega_X\omega_Y}, \quad \text{with} \quad \omega_Y = -\omega_X \tag{6}$$

between the second-order (with respect to the perturbation strength) time-averaged quasienergy $\{Q^{(2)}\}_T$ and the linear response function $\langle\langle X;Y\rangle\rangle_{\omega_X\omega_Y}$. The latter corresponds to the negative of frequency-dependent polarizability, if X and Y are position operators. Provided that the wave-function parameters $t_\mu(t)$ specifying $|\tilde{\Psi}(t)\rangle$ [gathered in the vector $t(t)$] are *variational*, i.e., they minimize $\{Q(t)\}_T$, the linear-response

function can be cast in the form [14,40]

$$\begin{aligned}\langle\langle X;Y\rangle\rangle_{\omega_X\omega_Y} &= \eta^X t^Y_{(\omega_Y)} + \eta^Y t^X_{(\omega_X)} + t^{X\dagger}_{(-\omega_X)}\eta^{Y\dagger} + t^{Y\dagger}_{(-\omega_Y)}\eta^{X\dagger} \\ &+ t^{X\dagger}_{(-\omega_X)}\mathbf{G}(\omega_Y)t^Y_{(\omega_Y)} + t^{Y\dagger}_{(-\omega_Y)}\mathbf{G}(\omega_X)t^X_{(\omega_X)} \\ &+ t^{X\dagger}_{(-\omega_X)}t^{Y\dagger}_{(-\omega_Y)}\mathbf{B}^\dagger + \mathbf{B}t^X_{(\omega_X)}t^Y_{(\omega_Y)}, \end{aligned} \tag{7}$$

with the vector η^X and the matrices $\mathbf{B}$ and $\mathbf{G}(\omega_Y)$ being defined as

$$\eta^X_\mu = \frac{\partial^2\{Q^{(2)}(t)\}_T}{\partial\epsilon_X(\omega_X)\partial t^{(1)}_\mu(\omega_Y)}, \quad \mathbf{G}_{\mu\nu}(\omega_Y) = \frac{\partial^2\{Q^{(2)}(t)\}_T}{\partial t^{(1)\dagger}_\mu(\omega_Y)\partial t^{(1)}_\nu(\omega_Y)},$$
$$\mathbf{B}_{\mu\nu} = \frac{\partial^2\{Q^{(2)}(t)\}_T}{\partial t^{(1)}_\mu(\omega_X)\partial t^{(1)}_\nu(\omega_Y)}. \tag{8}$$

Here, μ and ν are indices of the wave-function parameters $t(t)$ parametrizing $|\tilde{\Psi}(t)\rangle$, and the derivatives are taken at zero-field strength. In order to arrive at Eqs. (7) and (8) we have expanded the wave-function parameters $t(t)$ and $t^\dagger(t)$ in the Fourier components of the perturbation (1) as

$$\begin{aligned} t_\mu(t) &= t^{(0)}_\mu + t^{(1)}_\mu(t) + \cdots, \quad \text{with} \\ t^{(1)}_\mu(t) &= \sum_{k=-N}^{N} t^{(1)}_\mu(\omega_k)\exp(-i\omega_k t), \\ t^{(1)}_\mu(\omega_k) &= \sum_X \epsilon_X(\omega_k)t^X_{\mu(\omega_k)}, \\ t^\dagger_\mu(t) &= t^{(0)\dagger}_\mu + t^{(1)\dagger}_\mu(t) + \cdots, \quad \text{with} \\ t^{(1)\dagger}_\mu(t) &= \sum_{k=-N}^{N} t^{(1)\dagger}_\mu(-\omega_k)\exp(-i\omega_k t), \\ t^{(1)\dagger}_\mu(-\omega_k) &= \sum_X \epsilon_X(\omega_k)t^{X\dagger}_{\mu(-\omega_k)} \end{aligned} \tag{9}$$

[see also Eqs. (3.2)–(3.7) in Ref. [14], or Eq. (17) in Ref. [40]] and made use of the $2n+1$ rule.

Variationality of $\{Q(t)\}_T$ with respect to the wave-function parameters of $|\tilde{\Psi}(t)\rangle$ implies the stationary conditions

$$\begin{aligned} \frac{\partial\langle\langle X;Y\rangle\rangle_{\omega_X\omega_Y}}{\partial t^{X\dagger}_{(-\omega_X)}} &= \eta^{Y\dagger} + \mathbf{G}(\omega_Y)t^Y_{(\omega_Y)} + t^{Y\dagger}_{(-\omega_Y)}\mathbf{B}^\dagger \stackrel{!}{=} 0, \\ \frac{\partial\langle\langle X;Y\rangle\rangle_{\omega_X\omega_Y}}{\partial t^{X}_{(\omega_X)}} &= \eta^{Y} + t^{Y\dagger}_{(-\omega_Y)}\mathbf{G}(-\omega_Y) + \mathbf{B}t^Y_{(\omega_Y)} \stackrel{!}{=} 0, \end{aligned} \tag{10}$$

which specify the parameter responses t^Y. By virtue of Eq. (10), Eq. (7) simplifies to

$$\langle\langle X;Y\rangle\rangle_{\omega_X\omega_Y} = \langle\langle X;Y\rangle\rangle_{-\omega_Y\omega_Y} = \eta^X t^Y_{(\omega_Y)} + t^{Y\dagger}_{(-\omega_Y)}\eta^{X\dagger}. \tag{11}$$

Note that expression (11) for a polarizability at a given frequency ω_Y involves two independent sets of parameter responses $t^Y_{(\omega_Y)}$ and $t^{Y\dagger}_{(-\omega_Y)}$, which are obtained by solving the coupled linear equation system (10). However, when the $\mathbf{B}$ matrix is zero (*vide infra*), the equations for $t^Y_{(\omega_Y)}$ and $t^{Y\dagger}_{(-\omega_Y)}$ decouple.

The poles of $\langle\langle X;Y\rangle\rangle_{\omega_X\omega_Y}$ occur at frequencies ω_f, for which the parameter responses $t^Y_{(\omega_f)}$ become infinite, i.e., when the matrix

$$\begin{pmatrix} \mathbf{G}(\omega_f) & \mathbf{B}^* \\ \mathbf{B} & \mathbf{G}(\omega_f)^* \end{pmatrix} \tag{12}$$

is singular. This leads to a Casida-like eigenvalue problem [41] for the excitation energies ω_f,

$$\begin{pmatrix} \mathbf{A} & \mathbf{B}^* \\ \mathbf{B} & \mathbf{A}^* \end{pmatrix}\begin{pmatrix} U^f \\ U^{-f} \end{pmatrix} = \omega_f \begin{pmatrix} \mathbf{M} & \mathbf{0} \\ \mathbf{0} & -\mathbf{M}^* \end{pmatrix}\begin{pmatrix} U^f \\ U^{-f} \end{pmatrix}. \tag{13}$$

Here we have introduced the matrices $\mathbf{A}$ and $\mathbf{M}$ as components of $\mathbf{G}(\omega_Y)$:

$$\mathbf{G}(\omega_Y) = \mathbf{A} - \omega_Y\mathbf{M}, \tag{14}$$

where $\mathbf{A}$ is the ω-independent part of $\mathbf{G}$, and $\mathbf{M}$ is the metric matrix.

B. Time-dependent second-order variational coupled-cluster theory

The formalism for time-dependent second-order variational coupled-cluster (TD-VCC[2]) linear response has been explained in detail in Ref. [40] (Paper I). Here we just review the most relevant points, for comparison with time-dependent second-order unitary coupled-cluster theory (TD-UCC[2]) (*vide infra*). The wave function $|\tilde{\Psi}(t)\rangle$ has the form

$$|\tilde{\Psi}(t)\rangle = \exp[\mathbf{T}(t)]\,|0\rangle, \tag{15}$$

where $|0\rangle$ stands for the time-independent reference, i.e., the Hartree-Fock (HF) wave function. Furthermore,

$$\mathbf{T}(t) = \sum_i \mathbf{T}_i(t) = \sum_i\sum_{\mu_i} t_{\mu_i}(t)\tau_{\mu_i} \tag{16}$$

is the cluster operator with time-dependent amplitudes $t_{\mu_i}(t)$ (the wave-function parameters; *vide supra*), and corresponding (spin)orbital-replacement operators τ_{μ_i}, generating single- ($i=1$), double- ($i=2$), etc. (up to the actual number of electrons) orbital substitutions when acting on the HF reference. $\mathbf{T}_i(t)$, implicitly defined in (16), represents the i-fold excitation part of the cluster operator $\mathbf{T}(t)$.

Employing the wave-function *Ansatz* (15) variationally leads to the VCC theory. For the quasienergy, one obtains

$$Q(t) = \min_{t(t)} \frac{\langle 0|\exp[\mathbf{T}^\dagger(t)]\bar{\mathbf{H}}(t)\exp[\mathbf{T}(t)]|0\rangle}{\langle 0|\exp[\mathbf{T}^\dagger(t)]\exp[\mathbf{T}(t)]|0\rangle}. \tag{17}$$

The expression (17) contains disconnected diagrams and truncates only when the number of electrons is exhausted in the excitation. Although the Baker-Campbell-Hausdorff (BCH) expansion is not applicable here, this expression, as was shown by Cizek [48], can still be written in a fully connected form as

$$Q(t) = \min_{t(t)} \langle 0|\exp[\mathbf{T}^\dagger(t)]\bar{\mathbf{H}}(t)\exp[\mathbf{T}(t)]|0\rangle_C. \tag{18}$$

However, in this last expression exclusion-principle violating (EPV) terms are present [49], in which products of the cluster operators $\mathbf{T}_i$ are no longer restricted to the actual number of electrons, making the summations in (18) effectively infinite. Therefore, without further truncations, Eq. (18) is inapplicable.

In Paper I we have employed a *double perturbation theory* to devise TD-VCC[n] linear-response methods up to order $n=2$: In addition to the time-dependent perturbation $\mathbf{V}(t)$ [cf. Eq. (1)], the time-independent Hamiltonian $\mathbf{H}^{(0)}$ is partitioned (according to the standard Møller-Plesset partitioning) into the zeroth-order Fock operator $\mathbf{F}$, and the first-order fluctuation

potential $\mathbf{W}$, i.e.,

$$\mathbf{H}(t) = \mathbf{F}^{[0](0)} + \mathbf{W}^{[1](0)} + \mathbf{V}^{[0](1)}(t). \tag{19}$$

Here, and throughout the paper, the order with respect to the fluctuation potential is given in square brackets, while the order with respect to the time-dependent perturbation is given in parentheses.

The amplitudes (or formally, the corresponding cluster operators) can be expanded in orders with respect to both perturbation operators as

$$\begin{aligned}\mathbf{T}(t) = \mathbf{T}^{[1](0)} + \mathbf{T}^{[2](0)} + \cdots + \mathbf{T}^{[0](1)}(t) \\ + \mathbf{T}^{[1](1)}(t) + \mathbf{T}^{[2](1)}(t) + \cdots .\end{aligned} \tag{20}$$

The amplitudes, which are of zeroth order in $\mathbf{V}(t)$, are obviously time-independent. The expansion of the amplitudes in the Fourier components of the perturbation (1) as in Eq. (9), followed by the insertion into the respective TD-VCC[n] quasienergy and the time-averaging over the period T, yields the linear-response function by virtue of Eq. (6). Note that the time-dependent singles amplitudes in second-order TD-VCC[2] theory [40] are actually not partitioned into individual components of various $\mathbf{W}$ orders as in Eq. (20), but instead serve as parameters correct through second order (which is indicated by the superscript $[\leqslant 2]$ in $\mathbf{T}_1^{[\leqslant 2](1)}$)

$$\mathbf{T}^{[0](1)}(t) + \mathbf{T}^{[1](1)}(t) + \mathbf{T}^{[2](1)}(t) \Rightarrow \mathbf{T}^{[\leqslant 2](1)}. \tag{21}$$

The time-averaged TD-VCC[2] quasienergy $\{{}^{2n+1}Q^{[\leqslant 2](2)}\}_T$ is defined such that it collects all terms which are of exact second order with respect to the perturbation $\mathbf{V}$, and correct through second order with respect to the fluctuation potential $\mathbf{W}$. Furthermore, the $2n+1$ rule with respect to the perturbation $\mathbf{V}$ applies, as indicated by the corresponding superscript. The time-averaged TD-VCC[2] quasienergy is given explicitly in Eq. (41) of Paper I. The matrices $\mathbf{G}^{[\leqslant 2]}(\omega_Y)$, $\mathbf{B}^{[\leqslant 2]}$, and the vector $\eta^{Y[\leqslant 2]}$, the latter constituting the right-hand side of the stationary conditions [Eq. (10)], are obtained from $\{{}^{2n+1}Q^{[\leqslant 2](2)}\}_T$ according to Eq. (8), yielding

$$\begin{aligned}\eta^{Y[\leqslant 2]}_{\mu_i} = \langle 0|\big(\mathbf{1} + \mathbf{T}_1^{[2](0)\dagger} + \mathbf{T}_2^{[1](0)\dagger} + \mathbf{T}_2^{[2](0)\dagger}\big)\mathbf{Y}\tau_{\mu_1} \\ + \mathbf{T}_2^{[1](0)\dagger}\mathbf{Y}\mathbf{T}_2^{[1](0)}\tau_{\mu_1} + \mathbf{T}_2^{[1](0)\dagger}\mathbf{Y}\tau_{\mu_2}|0\rangle_C,\end{aligned} \tag{22}$$

$$\begin{aligned}\mathbf{G}^{[\leqslant 2]}_{\mu_i\nu_j}(\omega_Y) = \langle 0|\tau^\dagger_{\mu_1}\big(\mathbf{F} + \mathbf{T}_2^{[1](0)\dagger}\mathbf{F}\mathbf{T}_2^{[1](0)} + \mathbf{W} + \mathbf{W}\mathbf{T}_2^{[1](0)} \\ + \mathbf{T}_2^{[1](0)\dagger}\mathbf{W} - \omega_Y - \omega_Y\mathbf{T}_2^{[1](0)\dagger}\mathbf{T}_2^{[1](0)}\big)\tau_{\nu_1} \\ + \tau^\dagger_{\mu_1}\mathbf{W}\tau_{\nu_2} + \tau^\dagger_{\mu_2}\mathbf{W}\tau_{\nu_1} + \tau^\dagger_{\mu_2}(\mathbf{F} - \omega_Y)\tau_{\nu_2}|0\rangle_C,\end{aligned} \tag{23}$$

$$\mathbf{B}^{[\leqslant 2]} = 0. \tag{24}$$

In the above equations the superscript $[\leqslant 2]$ of $\mathbf{G}^{[\leqslant 2]}(\omega_Y)$, $\mathbf{B}^{[\leqslant 2]}$, and $\eta^{Y[\leqslant 2]}$ indicates that the corresponding object originates from the quasienergy, which is correct through second order with respect to $\mathbf{W}$. Correctness through second order, however, does not necessarily transfer to these objects, which are derivatives of the quasienergy. Since the $\mathbf{B}^{[\leqslant 2]}$ matrix in the TD-VCC[2] theory vanishes, the position of the poles of the linear response function, i.e., the excitation energies, can be obtained by solving the simplified [with respect to Eq. (13)] eigenvalue problem

$$\mathbf{A}U^f = \omega_f\mathbf{M}U^f, \tag{25}$$

which is Hermitian, provided that the $\mathbf{M}$ matrix is positive definite (see Sec. III E for discussion of this issue).

We note in passing, that the double perturbation theory as outlined above, can also be applied to the traditional non-Hermitian coupled-cluster method. As mentioned in Paper I (cf. Sec. IV E of Ref. [40]), the working equations of the resulting second-order method, denoted in the following as TD-CC[2], are equivalent to those of the CIS(D_∞) approach [21]. The latter does not originate from a linear response or EOM approach, but is an iterative version of the CIS method with the second-order correlation correction (D) [50].

C. TD-UCC[2]

Following the same lines, a linear-response method based on the UCC *Ansatz* [26,27] can be devised. The UCC wave function is defined as

$$|\tilde{\Psi}_{\mathrm{UCC}}(t)\rangle = \exp[\mathbf{T}(t) - \mathbf{T}^\dagger(t)]|0\rangle, \tag{26}$$

which has the nice property of being exponential and normalized at the same time. The time-dependent UCC quasienergy can then be written as the expectation value

$$\begin{aligned}Q(t) &= \min_{t(t)}\langle 0|\exp[-\mathbf{T}(t) + \mathbf{T}^\dagger(t)]\bar{\mathbf{H}}(t)\exp[\mathbf{T}(t) - \mathbf{T}^\dagger(t)]|0\rangle \\ &= \min_{t(t)}\langle 0|\bar{\mathbf{H}}(t) + [\bar{\mathbf{H}}(t),\mathbf{T}(t) - \mathbf{T}^\dagger(t)] \\ &\quad + \tfrac{1}{2}[[\bar{\mathbf{H}}(t),\mathbf{T}(t) - \mathbf{T}^\dagger(t)],\mathbf{T}(t) - \mathbf{T}^\dagger(t)] + \cdots|0\rangle,\end{aligned} \tag{27}$$

which now (and in contrast to TD-VCC) can be rewritten as a BCH commutator expansion. Yet it does not terminate after the fourfold-nested commutator as for traditional CC theory, and not even after the terms which exhaust the number of electrons. Similarly to the connected version of the VCC expression [cf. Eq. (18)], the summations in Eq. (27) are effectively infinite [28].

It is well known that commutators can be replaced by connected expressions, i.e.,

$$[\mathbf{O},\mathbf{T} - \mathbf{T}^\dagger] = (\mathbf{O}\mathbf{T})_C + (\mathbf{T}^\dagger\mathbf{O})_C; \tag{28}$$

hence the quasienergy expression [see Eq. (27)] can be recast in fully connected form as

$$\begin{aligned}Q(t) = \min_{\mathbf{t}(t)}\langle 0|\bar{\mathbf{H}}(t) + (\bar{\mathbf{H}}(t)\mathbf{T}(t))_C + (\mathbf{T}^\dagger(t)\bar{\mathbf{H}}(t))_C \\ + \tfrac{1}{2}\{(\mathbf{T}^\dagger(t)(\bar{\mathbf{H}}(t)\mathbf{T}(t))_C)_C + ((\bar{\mathbf{H}}(t)\mathbf{T}(t))_C\mathbf{T}(t))_C \\ + (\mathbf{T}^\dagger(t)(\mathbf{T}^\dagger(t)\bar{\mathbf{H}}(t))_C)_C + ((\mathbf{T}^\dagger(t)\bar{\mathbf{H}}(t))_C\mathbf{T}(t))_C\} + \cdots|0\rangle.\end{aligned} \tag{29}$$

The commutator involving the time-derivative part of $\bar{\mathbf{H}}$ appearing in Eq. (27) simplifies to

$$\begin{aligned}\left[\frac{\partial}{\partial t},\mathbf{T}(t) - \mathbf{T}^\dagger(t)\right] \\ = \left(\frac{\partial}{\partial t}\mathbf{T}(t)\right) - \left(\frac{\partial}{\partial t}\mathbf{T}^\dagger(t)\right) = \dot{\mathbf{T}}(t) - \dot{\mathbf{T}}^\dagger(t),\end{aligned} \tag{30}$$

where the parentheses imply that the time derivative has to be applied to the amplitudes of this cluster operator only (just the first term of the product rule survives, by virtue of the

commutator). Hence, we have

$$(\bar{\mathbf{H}}(t)\mathbf{T}(t))_C = (\mathbf{H}(t)\mathbf{T}(t))_C - i\dot{\mathbf{T}}(t) \quad \text{and}$$
$$(\mathbf{T}^\dagger(t)\bar{\mathbf{H}}(t))_C = (\mathbf{T}^\dagger(t)\mathbf{H}(t))_C + i\dot{\mathbf{T}}^\dagger(t), \tag{31}$$

for each of these terms occurring in Eq. (29). In the nested commutators, according to Eqs. (30) and (31), the time derivative only acts within the innermost commutator.

Since the UCC parametrization of the wave function (26) involves *noncommuting* $\mathbf{T}$ and $\mathbf{T}^\dagger$ operators, the exponential of a sum of time-dependent $\mathbf{T}^{(\geqslant 1)}(t)$,$\mathbf{T}^{(\geqslant 1)\dagger}(t)$ and time-independent $\mathbf{T}^{(0)}$,$\mathbf{T}^{(0)\dagger}$ cluster operators does not factorize into a product of two exponentials gathering the time-dependent and the time-independent pieces separately, as in the VCC or standard CC cases. Hence, in addition to the primary TD-UCC *Ansatz*

$$\left|\tilde{\Psi}^T_{\mathrm{UCC}}(t)\right\rangle = \exp\left((\mathbf{T}^{(0)} + \mathbf{T}^{(\geqslant 1)}(t)) - (\mathbf{T}^{(0)\dagger} + \mathbf{T}^{(\geqslant 1)\dagger}(t))\right)|0\rangle, \tag{32}$$

one can form alternative *Ansätze*, based on an enforced exponential factorization. The two most obvious forms of time-dependent UCC wave functions are

$$\left|\tilde{\Psi}^H_{\mathrm{UCC}}(t)\right\rangle = \exp(\mathbf{T}^{(0)} - \mathbf{T}^{(0)\dagger}) \exp\left(\mathbf{T}^{(\geqslant 1)}(t) - \mathbf{T}^{(\geqslant 1)\dagger}(t)\right)|0\rangle \tag{33}$$

and

$$\left|\tilde{\Psi}^D_{\mathrm{UCC}}(t)\right\rangle = \exp\left(\mathbf{T}^{(\geqslant 1)}(t) - \mathbf{T}^{(\geqslant 1)\dagger}(t)\right) \exp(\mathbf{T}^{(0)} - \mathbf{T}^{(0)\dagger})|0\rangle. \tag{34}$$

From Eq. (29) the time-averaged quasienergy $\{^{2n+1}Q^{(2)}\}_T$ can be devised for different orders with respect to the fluctuation potential $\mathbf{W}$. In zeroth order with respect to $\mathbf{W}$ the ground-state amplitudes do not contribute, making all three TD-UCC[0] *Ansätze* equivalent (the excitation energies are identical to the HF orbital energy differences, cf. Appendix A 1, as is the case for TD-VCC[0]). Yet already in first order with respect to $\mathbf{W}$ (TD-UCC[1]), the formalisms for the excitation energies and polarizabilities deviate for the three parametrizations presented in Eqs. (32)–(34). First we consider the TD-UCC-H *Ansatz* [see Eq. (33)], for which the quasienergy takes the form

$$\begin{aligned} Q^H(t) &= \left\langle \tilde{\Psi}^H_{\mathrm{UCC}}\middle|\bar{\mathbf{H}}\middle|\tilde{\Psi}^H_{\mathrm{UCC}}\right\rangle \\ &= \langle 0|\exp\left(-\mathbf{T}^{(\geqslant 1)}(t) + \mathbf{T}^{(\geqslant 1)\dagger}(t)\right)\exp(-\mathbf{T}^{(0)} + \mathbf{T}^{(0)\dagger})\bar{\mathbf{H}} \\ &\quad \times \exp(\mathbf{T}^{(0)} - \mathbf{T}^{(0)\dagger})\exp\left(\mathbf{T}^{(\geqslant 1)}(t) - \mathbf{T}^{(\geqslant 1)\dagger}(t)\right)|0\rangle. \end{aligned} \tag{35}$$

The BCH expansion for the inner exponentials involving the ground-state amplitudes has to be performed first, which is then subject to the second BCH expansion with the exponentials of the time-dependent operators, as sketched in Appendix A 1. The time-dependent rotation of the ground-state similarity-transformed Hamiltonian matrix in (35) resembles the EOM-UCC scheme, and in fact, agrees with the latter in all orders of the time-dependent perturbation [see Eq. (38) of Ref. [51]]. Such a factorization of the wave function, where the time-independent amplitudes are forming the innermost commutators, leads to an important simplification for the time-derivative part of $\bar{\mathbf{H}}$,

$$\begin{aligned} \left\langle \tilde{\Psi}^H_{\mathrm{UCC}}\middle|i\frac{\partial}{\partial t}\middle|\tilde{\Psi}^H_{\mathrm{UCC}}\right\rangle &= \langle 0|\exp\left(-\mathbf{T}^{(>0)}(t) + \mathbf{T}^{(>0)\dagger}(t)\right)\left(i\frac{\partial}{\partial t}\right) \\ &\quad \times \exp\left(\mathbf{T}^{(>0)}(t) - \mathbf{T}^{(>0)\dagger}(t)\right)|0\rangle. \end{aligned} \tag{36}$$

Any contribution from the time-independent ground-state amplitudes in the first BCH expansion is zeroed by the time derivative of the amplitudes in the innermost commutator [see Eqs. (30) or (31)]. This implies that in contrast to the TD-VCC method, and also in contrast to the other parametrizations of TD-UCC (*vide supra*) the metric matrix $\mathbf{M}$ is just the identity matrix at any $\mathbf{W}$ order of the TD-UCC-H formalism (cf. Appendix A 2).

It is shown in detail in Appendix A 1 that the working equations for the TD-UCC[1]-H excitation energies are equivalent to those of TD-VCC[1] [40]. This means that the $\mathbf{B}$ matrix vanishes and the Jacobian corresponds to a Hermitian CIS matrix. On the other hand, the η term, and, thus the polarizabilities of TD-UCC[1]-H, similarly to the TD-VCC[1] case, are not equal to those of CIS, but rather correspond to ADC(1) [see Eq. (45b) of Ref. [52]]. For the TD-UCC-H method the $\mathbf{B}$ matrix vanishes also for higher orders in $\mathbf{W}$. Hence the simplified Hermitian eigenvalue problem [see Eq. (25)] is recovered also for higher orders in $\mathbf{W}$, just as is the case for TD-VCC (cf. Paper I). Such an observation was already reported in an early paper on the UCC parametrization of the wave function within the polarization propagator formalism [53].

Writing out the commutators of the double BCH expansion of TD-UCC-H (Appendix A 1) and keeping only those terms second order in $\mathbf{V}$, and up to second order in $\mathbf{W}$, one finally arrives after time averaging at the following expression for the TD-UCC[2]-H quasienergy,

$$\begin{aligned} \{^{2n+1}Q^{[\leqslant 2](2)}\}_T = \sum_k \langle 0|&\frac{1}{2}\mathbf{T}^{[\leqslant 2](1)\dagger}_{1(-\omega_k)}\mathbf{T}^{[\leqslant 2](1)\dagger}_{1(\omega_k)}\left[\mathbf{F}\left(\mathbf{T}^{[1](0)}_2 + \mathbf{T}^{[2](0)}_2\right) + \mathbf{W} + \mathbf{W}\mathbf{T}^{[1](0)}_2\right]_C + \frac{1}{2}\left[\left(\mathbf{T}^{[1](0)\dagger}_2 + \mathbf{T}^{[2](0)\dagger}_2\right)\mathbf{F}\right. \\ &\left. + \mathbf{W} + \mathbf{T}^{[1](0)\dagger}_2\mathbf{W}\right]_C\mathbf{T}^{[\leqslant 2](1)}_{1(-\omega_k)}\mathbf{T}^{[\leqslant 2](1)}_{1(\omega_k)} + \mathbf{T}^{[\leqslant 2](1)\dagger}_{1(\omega_k)}\left(\mathbf{F} + \mathbf{W} + \frac{1}{2}\mathbf{W}\mathbf{T}^{[1](0)}_2 + \frac{1}{2}\mathbf{T}^{[1](0)\dagger}_2\mathbf{W}\right)_C\mathbf{T}^{[\leqslant 2](1)}_{1(\omega_k)} \\ &+ \mathbf{T}^{[1](1)\dagger}_{2(\omega_k)}\mathbf{F}\mathbf{T}^{[1](1)}_{2(\omega_k)} + \mathbf{T}^{[\leqslant 2](1)\dagger}_{1(\omega_k)}\mathbf{W}\mathbf{T}^{[1](1)}_{2(\omega_k)} + \mathbf{T}^{[1](1)\dagger}_{2(\omega_k)}\mathbf{W}\mathbf{T}^{[\leqslant 2](1)}_{1(\omega_k)} - \omega_k\left(\mathbf{T}^{[\leqslant 2](1)\dagger}_{1(\omega_k)}\mathbf{T}^{[\leqslant 2](1)}_{1(\omega_k)} + \mathbf{T}^{[1](1)\dagger}_{2(\omega_k)}\mathbf{T}^{[1](1)}_{2(\omega_k)}\right) \\ &+ \mathbf{T}^{[\leqslant 2](1)\dagger}_{1(\omega_k)}\mathbf{V}^{\omega_k}\left(\mathbf{1} + \mathbf{T}^{[2](0)}_1 + \mathbf{T}^{[1](0)}_2 + \mathbf{T}^{[2](0)}_2\right) + \left(\frac{1}{2}\mathbf{T}^{[\leqslant 2](1)\dagger}_{1(\omega_k)}\mathbf{T}^{[1](0)\dagger}_2 + \mathbf{T}^{[1](1)\dagger}_{2(\omega_k)}\right)\mathbf{V}^{\omega_k}\mathbf{T}^{[1](0)}_2 \\ &+ \mathbf{T}^{[1](0)\dagger}_2\mathbf{V}^{-\omega_k}\left(\frac{1}{2}\mathbf{T}^{[1](0)}_2\mathbf{T}^{[\leqslant 2](1)}_{1(\omega_k)} + \mathbf{T}^{[1](1)}_{2(\omega_k)}\right) + \left(\mathbf{1} + \mathbf{T}^{[2](0)\dagger}_1 + \mathbf{T}^{[1](0)\dagger}_2 + \mathbf{T}^{[2](0)\dagger}_2\right)\mathbf{V}^{-\omega_k}\mathbf{T}^{[\leqslant 2](1)}_{1(\omega_k)}|0\rangle_C, \end{aligned} \tag{37}$$

where the superscript $2n+1$ again indicates that the $2n+1$ rule (with respect to $\mathbf{V}$) applies. Furthermore, the MP2 equations are utilized to cancel some of the terms, as is shown in Appendix A 3. Note that in particular, no product terms involving ω_k and *time-independent amplitudes* do occur, as is the case for TD-VCC[2] [cf. Eq. (41) in Paper I]. The metric matrix $\mathbf{M}$ therefore is just the identity matrix, as already stated above.

Expressions for the matrices $\mathbf{G}^{[\leqslant 2]}(\omega_Y)$, $\mathbf{B}^{[\leqslant 2]}$, and the vector $\eta^{Y[\leqslant 2]}$ are obtained by differentiating $\{^{2n+1}Q^{[\leqslant 2](2)}\}_T$ according to Eq. (8),

$$\eta^{Y[\leqslant 2]}_{\mu_i} = \langle 0|\big(\mathbf{1} + \mathbf{T}_1^{[2](0)\dagger} + \mathbf{T}_2^{[1](0)\dagger} + \mathbf{T}_2^{[2](0)\dagger}\big)\mathbf{Y}\tau_{\mu_1} + \tfrac{1}{2}\mathbf{T}_2^{[1](0)\dagger}\mathbf{Y}\mathbf{T}_2^{[1](0)}\tau_{\mu_1} + \mathbf{T}_2^{[1](0)\dagger}\mathbf{Y}\tau_{\mu_2}|0\rangle_C, \quad (38)$$

$$\mathbf{G}^{[\leqslant 2]}_{\mu_i\nu_j}(\omega_Y) = \langle 0|\tau^\dagger_{\mu_1}\big(\mathbf{F} + \mathbf{W} + \tfrac{1}{2}\mathbf{W}\mathbf{T}_2^{[1](0)} + \tfrac{1}{2}\mathbf{T}_2^{[1](0)\dagger}\mathbf{W} - \omega_Y\big)\tau_{\nu_1} + \tau^\dagger_{\mu_1}\mathbf{W}\tau_{\nu_2} + \tau^\dagger_{\mu_2}\mathbf{W}\tau_{\nu_1} + \tau^\dagger_{\mu_2}(\mathbf{F} - \omega_Y)\tau_{\nu_2}|0\rangle_C, \quad (39)$$

$$\mathbf{B}^{[\leqslant 2]}_{\mu_i\nu_j} = \langle 0|\big(\mathbf{T}_2^{[1](0)\dagger}\mathbf{F} + \mathbf{W} + \mathbf{T}_2^{[2](0)\dagger}\mathbf{F} + \mathbf{T}_2^{[1](0)\dagger}\mathbf{W}\big)\tau_{\mu_1}\tau_{\nu_1}|0\rangle_C = 0. \quad (40)$$

Comparing Eqs. (39) and (23), it can be seen that the TD-VCC[2] terms $\langle 0|\tau_{\mu_1}\mathbf{T}_2^{[1](0)\dagger}\mathbf{T}_2^{[1](0)}\tau_{\nu_1}|0\rangle_C$ in the $\mathbf{M}$ matrix and $\langle 0|\tau_{\mu_1}\mathbf{T}_2^{[1](0)\dagger}\mathbf{F}\mathbf{T}_2^{[1](0)}\tau_{\nu_1}|0\rangle_C$ in the $\mathbf{A}$ matrix either do not appear (the former, cf. Appendix A 2) or cancel out (the latter, cf. Appendix A 3) in the TD-UCC[2]-H method. Finally, as the last equality of Eq. (40) shows, the $\mathbf{B}$ matrix of the TD-UCC[2]-H method indeed vanishes, under the assumption that the ground-state MP2 and MP3 equations are satisfied. Hence the TD-UCC[2]-H Jacobian is Hermitian, and only the simplified Hermitian eigenvalue problem [see Eq. (25)] has to be solved to obtain excitation energies and eigenstates.

A direct comparison reveals that the equations for the excitation energies and polarizabilities of the TD-UCC[2]-H method are equivalent to those of the ADC(2) method [52,54] [the η terms of ADC(2) are given in Eq. (54) of Ref. [52]; the Jacobian of ADC(2) can be found in Ref. [21], Eqs. (6) and (7)]. A close relation between UCC and ADC methods has already been mentioned before [55,56]. In particular, in Ref. [55] it was shown that a polarization-propagator formalism based on a perturbative UCC *Ansatz*, where the UCC-H form of the wave-function parametrization is actually automatically realized, yields the same expressions as ADC. In this work we have shown that this connection also exists within one of the formulations of TD-UCC linear response, namely, the H parametrization, and we have worked this out in detail for the second-order method with respect to the fluctuation potential $\mathbf{W}$.

For the D parametrization of the TD-UCC wave function [see Eq. (34)], the quasienergy also calls for a double BCH expansion, but in the opposite order: here, the innermost part is time dependent. Interestingly, this method has some connection to density-matrix-based time-dependent theories. Indeed, introducing the resolution of identity $\sum_I |I\rangle\langle I|$, one can rewrite the pure Hamiltonian part of the TD-UCC-D quasienergy (i.e., without the time derivative) as

$$\big\langle\tilde\Psi^D_{\mathrm{UCC}}\big|\mathbf{H}\big|\tilde\Psi^D_{\mathrm{UCC}}\big\rangle = \big\langle\Psi^{(0)}_{\mathrm{UCC}}\big|\exp\left(\mathbf{T}^{(\geqslant 1)\dagger}(t) - \mathbf{T}^{(\geqslant 1)}(t)\right)\sum_I |I\rangle\langle I|\mathbf{H}\sum_J |J\rangle\langle J|\exp\left(\mathbf{T}^{(\geqslant 1)}(t) - \mathbf{T}^{(\geqslant 1)\dagger}(t)\right)\big|\Psi^{(0)}_{\mathrm{UCC}}\big\rangle$$
$$= \mathrm{tr}\left\{\sum_J \langle I|\mathbf{H}|J\rangle\langle J|\exp\left(\mathbf{T}^{(\geqslant 1)}(t) - \mathbf{T}^{(\geqslant 1)\dagger}(t)\right)\big|\Psi^{(0)}_{\mathrm{UCC}}\big\rangle\big\langle\Psi^{(0)}_{\mathrm{UCC}}\big|\exp\left(\mathbf{T}^{(\geqslant 1)\dagger}(t) - \mathbf{T}^{(\geqslant 1)}(t)\right)|I'\rangle\right\}. \quad (41)$$

This expression can be interpreted as the trace of the Hamiltonian contracted with the matrix of the ground-state many-electron density projection operator $|\Psi^{(0)}_{\mathrm{UCC}}\rangle\langle\Psi^{(0)}_{\mathrm{UCC}}|$ rotated by a time-dependent unitary transformation operator. As a practical example to illustrate this connection we consider the TD-UCC[1]-D method. In Appendix A 1 we demonstrate that the TD-UCC[1]-D formalism is equivalent to TD-HF, which can also be regarded as a HF density-matrix response theory [57–59]. Interestingly, this equivalence holds not only for the excitation energies, but also for the polarizabilities, i.e., unlike TD-VCC[1], TD-UCC[1]-H, or ADC(1), the $\mathbf{B}$ matrix of TD-UCC[1]-D does not vanish, but, at the same time, the η-term does not include any terms involving the ground-state amplitudes.

Finally, the general TD-UCC-T scheme involves a single BCH expansion leading to Eqs. (27) and (29). As demonstrated in Appendix A 1, the first-order method (with respect to $\mathbf{W}$), i.e., TD-UCC[1]-T, has a nonzero $\mathbf{B}$ matrix, but it is weighted with a factor of $\frac{1}{2}$ relative to that of TD-UCC[1]-D. The resulting eigenvalue problem for the TD-UCC[1]-T excitation energies hence corresponds to kind of an average between TD-UCC[1]-D and TD-UCC[1]-H ($\mathbf{B} = 0$), or equivalently, between TD-HF and its Tamm-Dancoff approximation. Such an average also holds for the η term of the TD-UCC-T method and therefore for the polarizabilities.

For the second-order methods TD-UCC[2]-D and TD-UCC[2]-T the $\mathbf{B}$ block does not vanish, rendering the Jacobian as non-Hermitian, and the full Casida-like eigenvalue problem (13) has to be solved. Furthermore, the metric matrix $\mathbf{M}$ is not just an identity matrix as in TD-UCC[2]-H. For these reasons, the formalisms of TD-UCC[2]-D and TD-UCC[2]-T are more complex than that of TD-UCC[2]-H and are not considered further in the present work. Investigation and corresponding numerical results for these two *Ansätze* are planned for a forthcoming publication. Below we focus on the Hermitian-Jacobian TD-VCC[2] and TD-UCC[2]-H [=ADC(2)] theories. For the latter, we drop the postfix "-H" in the following for convenience.

III. RESULTS AND DISCUSSION

A. Computational details

In the course of this work the TD-VCC[2] and TD-UCC[2] [=ADC(2)] methods have been implemented in the actual development version of MOLPRO [60,61], i.e., in the framework of our local Laplace-based [62] CC2 response method [63,64] and of the EOM-CC module [65]. In the following we compare TD-VCC[2] and TD-UCC[2] excitation energies and frequency-dependent polarizabilities (FDPs) to other methods. Most calculations were performed with MOLPRO; for the TD-CC2 and TD-CCSD FDPs, as well as the TD-CC3 excitation energies, the DALTON program [66] was employed. Static orbital-relaxed polarizabilities at the CCSD and the CCSD(T) level were computed via the finite-field technique.

As test molecules (i) water, (ii) formamide, and (iii) aniline were selected, which represent, respectively, (i) a simple case without double bonds, (ii) a case with an isolated double bond, and (iii) an aromatic molecule, respectively. As a further test molecule (just for excitation energies) the 1-phenylpyrrole molecule was chosen, which represents a more complicated organic molecule with two rings separated by a single C-C bond, featuring excited charge-transfer (CT) states shifting density from one ring to the other.

The geometries of the water, formamide, and aniline molecules were optimized at the level of MP2 in the cc-pVTZ atomic orbital (AO) basis, while the geometry of the 1-phenylpyrrole molecule was adopted from Ref. [65]. The excitation energy and FDP calculations were performed in the aug-cc-pVTZ (water, formamide), and the aug-cc-pVDZ (aniline, 1-phenylpyrrole) basis sets [67]. The core electrons (1*s* for C, O, and N) were excluded from the correlation treatment (frozen core approximation) in all calculations.

Furthermore, the additive separability of the excitation energies has been tested for the case of the BeH_2 molecule (aug-cc-pVTZ basis). The BeH_2 system has been used before for the same purpose, e.g., in Refs. [68,69].

B. Excitation energies

Table I compiles the TD-VCC[2] and TD-UCC[2] [=ADC(2)] vertical excitation energies for several lowest electronic singlet states of the four test molecules, which are compared to the corresponding TD-CC2 and TD-CCSD (=EOM-CCSD) values. For water and formamide, the TD-CC3 excitation energies are also included. The TD-CC[2] [=CIS(D_∞)] excitation energies differ from TD-UCC[2] at most by 0.001 eV for all states considered here (actually, this difference is usually even smaller) and are therefore omitted in the table. The discrepancies in the excitation energies of TD-CC2 and TD-CCSD vary substantially from state to state, but are for most cases not larger than 0.2 eV. Exceptions are two higher excited states of formamide (2 A' and 3 A' states; cf. third and fourth states in Table I) with a deviation as large as 0.7 eV. Apparently, relative to the more accurate TD-CC3 method, TD-CCSD overestimates the excitation energies of these states somewhat, but nevertheless, the error of TD-CC2 vs TD-CC3 is still quite large for these two problematic states, i.e., $\sim$0.4 eV. It should also be noted that the identification of corresponding states between TD-CC2 and TD-CCSD is unambiguous only for some (usually the few lowest) of the states: Indeed, the overlaps of the singles parts of the respective eigenfunctions of the CC Jacobian with CIS wave functions may be quite different for "corresponding" TD-CC2 and TD-CCSD states. Exactly such a situation occurs for the problematic A' states of formamide; the comparison between TD-CC2 and TD-CCSD thus has to be taken with a grain of salt for these states. For aniline, the TD-CC2 and TD-CCSD excitation energies agree within 0.2 eV for all states considered. The observed deviations between TD-CC2 and higher-order methods as employed in the present work are well in line with a recent study on excited states in nucleobases [70].

The TD-UCC[2] excitation energies are slightly lower than those of TD-CC2, although usually by only $\sim$0.05 eV (with the exception of the lowest state of formamide, where this difference is $\sim$0.2 eV). Such discrepancies are anticipated for second-order methods sharing a similar structure of the Jacobian, but differing in the ground-state reference (MP2 versus CC2).

The TD-VCC[2] excitation energies, on the other hand, exhibit a markedly larger deviation from those of the other two second-order methods. These differences typically amount to $\sim$0.2 eV, but there are several cases with larger deviations, e.g., 0.7 eV for the first excited state of formamide, or 0.5 eV for the first excited state of aniline, etc. Interestingly, the TD-VCC[2] excitation energies are *consistently lower* than those of the other second-order methods. Since the latter in turn systematically underestimate the TD-CCSD or TD-CC3 reference excitation energies, TD-VCC[2] is particularly bad for excitation energies, i.e., worse than TD-CC2 and TD-UCC[2]. Possible reasons for this failure of TD-VCC[2] are analyzed in detail in Sec. III E. Here, we only note that the relevant singles-singles block of the TD-VCC[2] Jacobian indeed deviates already in second order (with respect to $\mathbf{W}$) from the TD-UCC[2] or TD-CC[2] ones, even though it is correct through second order within the TD-VCC framework. The inherent problems of TD-VCC[2] regarding excitation energies are further illustrated by the CT states of 1-phenylpyrrole: Here, the highest occupied molecular orbital resides on the pyrrole ring, while the lowest unoccupied molecular orbital is located primarily on the phenol ring. Due to this feature, low-energy CT states are prominent in its spectrum. Indeed, for TD-CCSD, TD-CC2, and TD-UCC[2] the excited states 4, 7, and 8 possess partial CT character. On the other hand, for TD-VCC[2] no states with partial pyrrole to phenol excitation were found up to states 7 and 8. Also, the CIS overlap analysis (*vide supra*) reveals that the excitation characters of state 4 vary between TD-VCC[2] and the other methods.

C. Polarizabilities

In this section we explore how the different methods perform for the FDP at frequencies away from the poles. Table II compiles the FDPs for the two frequencies $\omega = 0.0$ a.u. (static) and $\omega = 0.1$ a.u., calculated using TD-VCC[2], TD-UCC[2], TD-CC2, and TD-CCSD methods. A much wider set of methods is tested in Appendix C. From numerical experience [71] it is known that the TD-CCSD method is the first one in the hierarchy of the TD-CCS, TD-CC2, TD-CCSD,

TABLE I. Excitation energies of the lowest singlet excited states of water, formamide, aniline, and 1-phenylpyrrole (in eV). In parentheses the deviation with respect to the reference (TD-CC3 in case of water and formamide, TD-CCSD for aniline and 1-phenylpyrrole) is given. Point symmetry of excited states of water: 1,4,6–B_1; 2–A_2; 3,5–A_1. Point symmetry of excited states of formamide: 1,2,5–A''; 3,4,6–A'.

Method	State 1	State 2	State 3	State 4	State 5	State 6	State 7	State 8
Molecule				Water				
TD-VCC[2]	7.01(−0.60)	8.69(−0.70)	9.40(−0.61)	10.17(−0.67)	10.68(−0.70)	10.83(−0.68)		
TD-UCC[2]	7.18(−0.43)	8.85(−0.54)	9.56(−0.45)	10.32(−0.52)	10.83(−0.55)	10.97(−0.54)		
TD-CC2	7.23(−0.38)	8.90(−0.49)	9.62(−0.39)	10.37(−0.47)	10.91(−0.47)	11.02(−0.49)		
TD-CCSD	7.60(−0.01)	9.37(−0.02)	10.00(−0.01)	10.81(−0.03)	11.37(−0.01)	11.49(−0.02)		
TD-CC3	7.61	9.39	10.01	10.84	11.38	11.51		
Molecule				Formamide				
TD-VCC[2]	4.94(−0.71)	6.54(−0.29)	6.08(−0.65)	6.65(−0.74)	7.35(−0.33)	7.00(−0.62)		
TD-UCC[2]	5.44(−0.21)	6.73(−0.10)	6.25(−0.48)	6.83(−0.56)	7.53(−0.15)	7.31(−0.31)		
TD-CC2	5.68(+0.03)	6.74(−0.09)	6.31(−0.42)	6.89(−0.50)	7.54(−0.14)	7.36(−0.26)		
TD-CCSD	5.69(+0.04)	6.91(+0.08)	6.99(+0.26)	7.55(+0.16)	7.76(+0.08)	7.78(+0.16)		
TD-CC3	5.65	6.83	6.73	7.39	7.68	7.62		
Molecule				Aniline				
TD-VCC[2]	4.25(−0.53)	4.63(−0.37)	5.21(−0.45)	5.32(−0.43)	5.36(−0.49)	5.98(−0.40)		
TD-UCC[2]	4.74(−0.04)	4.83(−0.17)	5.45(−0.21)	5.54(−0.21)	5.67(−0.18)	6.15(−0.23)		
TD-CC2	4.75(−0.03)	4.83(−0.17)	5.45(−0.21)	5.54(−0.21)	5.71(−0.14)	6.15(−0.23)		
TD-CCSD	4.78	5.00	5.66	5.75	5.85	6.38		
Molecule				1-phenylpyrrole				
TD-VCC[2]	4.39(−0.55)	4.80(−0.69)	5.13(−0.48)	5.27(−0.45)	5.28(−0.51)	5.43(−0.62)	5.67(−0.47)	5.71(−0.48)
TD-UCC[2]	4.91(−0.03)	5.27(−0.22)	5.46(−0.15)	5.47(−0.25)	5.53(−0.26)	5.78(−0.27)	5.85(−0.29)	5.90(−0.29)
TD-CC2	4.92(−0.02)	5.31(−0.18)	5.43(−0.18)	5.49(−0.23)	5.49(−0.30)	5.73(−0.32)	5.85(−0.29)	5.92(−0.27)
TD-CCSD	4.94	5.49	5.61	5.72	5.79	6.05	6.14	6.19

and TD-CC3 models, which usually yields rather accurate polarizabilities; thus this method serves as the benchmark in Table II. Apparently, for FDPs at frequencies away from the poles, TD-VCC[2] performs significantly better than for excitation energies; all three second-order methods are comparable and provide similar accuracy, which is in line with the theoretical considerations made in Paper I: The stationary conditions of TD-VCC[2] differ from those of

TABLE II. Dipole polarizabilities of water, formamide, and aniline (all values in a.u.). In parentheses the deviation with respect to TD-CCSD is given.

Method	α_{xx}		α_{yy}		α_{zz}		α_{yz}[a] or α_{xz}[b]	
Frequency	0.0	0.1	0.0	0.1	0.0	0.1	0.0	0.1
Molecule				Water				
TD-VCC[2]	9.59(0.51)	10.16(0.63)	10.47(0.50)	10.77(0.54)	10.08(0.63)	10.46(0.69)		
TD-UCC[2]	9.48(0.40)	10.01(0.48)	10.38(0.41)	10.67(0.44)	9.98(0.53)	10.35(0.58)		
TD-CC2	9.79(0.71)	10.36(0.83)	10.51(0.54)	10.80(0.57)	10.06(0.61)	10.43(0.66)		
TD-CCSD	9.08	9.53	9.97	10.23	9.45	9.77		
Molecule				Formamide				
TD-VCC[2]	21.03(0.80)	21.91(0.92)	29.21(1.91)	30.83(2.32)	41.01(4.48)	44.63(5.67)	1.69(0.84)	1.87(1.00)
TD-UCC[2]	20.86(0.63)	21.68(0.69)	28.87(1.57)	30.38(1.87)	39.98(3.45)	43.14(4.18)	1.64(0.79)	1.81(0.94)
TD-CC2	21.03(0.80)	21.88(0.89)	29.46(2.16)	31.08(2.57)	39.57(3.04)	42.56(3.60)	1.12(0.27)	1.23(0.36)
TD-CCSD	20.23	20.99	27.30	28.51	36.53	38.96	0.85	0.87
Molecule				Aniline				
TD-VCC[2]	53.66(2.20)	56.50(2.60)	94.37(7.42)	103.93(10.27)	114.09(10.53)	128.88(15.28)	−0.10(−0.18)	−0.31(−0.28)
TD-UCC[2]	53.26(1.80)	55.93(2.03)	92.85(5.90)	100.97(7.31)	111.30(7.74)	123.73(10.13)	−0.06(−0.14)	−0.22(−0.19)
TD-CC2	52.83(1.37)	55.51(1.61)	90.99(4.04)	98.62(4.96)	110.16(6.60)	122.05(8.45)	0.05(−0.03)	−0.09(−0.06)
TD-CCSD	51.46	53.90	86.95	93.66	103.56	113.60	0.08	−0.03

[a]For formamide.
[b]For aniline.

TD-CC[2] in the third order (with respect to **W**) only, which should lead to similar results for second-order properties for frequencies far from the poles. Furthermore, we note that all three second-order methods systematically overestimate the FDPs by several percent relative to the TD-CCSD benchmark. The influence of the nearest pole on the FDPs can be seen by comparing the increments in the FDPs on going from $\omega = 0.0$ a.u. to 0.1 a.u. It is largest for aniline (which has the lowest excitation energy), and of all methods applied to this molecule the TD-VCC[2] approach produces the largest error due to the underestimation of the excitation energies in this model, as discussed in the previous section.

D. Size extensivity, additive separability, and charge transfer

To deliver meaningful results for large systems, size extensivity (size intensivity for excitation energies) is a crucial property for a method. The expressions for the quasienergy are fully connected for all three methods TD-CC, TD-UCC, and TD-VCC. For TD-CC and TD-UCC this is a consequence of the BCH commutator expansion of the quasienergy expression [cf. Eqs. (27) and (29) for TD-UCC], while for TD-VCC the cancellation of the denominator leads to the connected form, cf. Eq. (18). Size extensivity of the quasienergy, however, does not guarantee that after differentiation with respect to the time-dependent amplitudes (and/or Lagrange multipliers in the case of TD-CC) the stationary conditions or the Jacobian are free of disconnected terms.

The stationary conditions for the amplitudes of the traditional TD-CC formalism contain only connected terms. Disconnected terms appear only in the stationary conditions for the Lagrange multipliers; however, due to the $2n + 2$ rule [14] they do not affect the linear response function, and thus the size extensivity of the TD-CC polarizabilities is not destroyed. The TD-CC Jacobian can also contain disconnected terms, but only in the upper-triangle part, which therefore cannot violate the size intensivity of the excitation energies [72]. TD-VCC, on the other hand, which has a Hermitian Jacobian, is more problematic in this respect. However, as was shown in Paper I, for the second-order TD-VCC[2] method disconnected terms occur neither in the stationary conditions, nor in the Jacobian. Finally, for the TD-UCC-*H* method with the time-dependent amplitudes appearing only in the second, outer BCH expansion, Eq. (35) implies only connected terms in both the stationary conditions, and the Jacobian, for arbitrary orders in **W**. Consequently, all the methods employed in the context of the present work are size extensive for polarizabilities, and size intensive for excitation energies.

Another important issue is the correct description of extensive properties in the asymptotic limit of noninteracting subsystems, i.e., the so-called additive separability: Electronic excitations from one subsystem (donor) to the other (acceptor) should be, in the noninteracting limit, equal to the sum of the corresponding ionization potential (IP) and electron affinity (EA) of the donor and the acceptor subsystems, respectively. For finite distances R between donor and acceptor subsystems, this sum has to be corrected by the Coulomb interaction $-\frac{1}{R}$ (in hartree) between the two charged fragments.

The additive separability of excited states is investigated for various methods on the example of the BeH_2 molecule. To this end this molecule is separated into two subsystems consisting of Be and H_2, with Be lying on the perpendicular bisector of the H_2 bond. The bond length in H_2 is kept fixed at 1.4 a.u. The necessary IPs and EAs were calculated with the corresponding program for the excitation energies, where ionized or electron-attached states are introduced into the spectrum by adding a single, very diffuse Gaussian orbital to the orbital basis set [73–76]. This is a very useful trick, since presently IPs and EAs are only available for TD-CC2 and TD-CC[2] within the MOLPRO code.

From Table III it can be seen that the difference $\mathrm{EE} - (\mathrm{IP} + \mathrm{EA} - \frac{1}{R})$ stabilizes at < 0.03 eV for all cases for the selected CT state of BeH_2. This value is several orders of magnitude smaller than the accuracy of methods, therefore we can conclude that all methods presented here are approximately additively separable. It should be noted that the exact separability would require switching, e.g., to Fock-space CC theory [69,77].

If we compare the values for the charge-transfer excitation energies themselves, there is evidently a relatively large error of all the second-order methods compared to the TD-CCSD benchmark. At a relatively small donor-acceptor distance of $R = 10$ bohrs the TD-VCC[2] excitation energy is below the TD-CC2 or TD-UCC[2] values by ~ 0.1 eV, i.e., somewhat less than for the states studied in Sec. III B. On the other hand, the discrepancy between TD-CC2 and TD-CCSD is considerably larger than the average difference in Table I.

Furthermore, for larger distances R, the deviation between the individual second-order methods vanishes entirely. Although many terms specific to the TD-VCC[2] Jacobian, i.e., of the type $\langle 0|\tau_{\mu_1}\mathbf{T}_2^{[1](0)\dagger}\mathbf{F}\mathbf{T}_2^{[1](0)}\tau_{\nu_1}|0\rangle_C$ in the **A** matrix, and $\langle 0|\tau_{\mu_1}\mathbf{T}_2^{[1](0)\dagger}\mathbf{T}_2^{[1](0)}\tau_{\nu_1}|0\rangle_C$ in the **M** matrix [see Eq. (23)], give a zero contribution to the long-range CT states, some of them do not decay at any distance R. Apparently, the influence of such terms on the excitation energies in the **A** matrix is counterbalanced by the corresponding **M**-matrix terms.

TABLE III. First excitation energy of the CT type and corresponding differences to the sum over ionization potential (Be) and electron affinity (H_2) corrected by the Coulomb attraction. The values for the distances and energies are given in bohrs and eV, respectively.

R	TD-CCSD	TD-CC2	TD-UCC[2]	TD-CC[2]	TD-VCC[2]
			Excitation energies		
10	8.812	8.186	8.207	8.207	8.108
20	9.304	8.968	8.989	8.989	8.957
50	10.125	9.726	9.749	9.749	9.745
100	10.397	9.993	10.015	10.015	10.019
1000	10.642	10.232	10.254	10.254	10.265
			$\mathrm{EE} - (\mathrm{IP} + \mathrm{EA} - \frac{1}{R})$		
10	0.889	0.671	0.671	0.671	0.559
20	0.021	0.092	0.093	0.093	0.047
50	0.025	0.034	0.036	0.036	0.019
100	0.025	0.029	0.030	0.030	0.021
1000	0.025	0.023	0.024	0.024	0.022

E. Behavior of the perturbative expansions

The previous sections show that the TD-VCC[2] method performs similarly as the other second-order methods for FDPs at frequencies sufficiently far from the poles, yet the underestimation of excitation energies (relative to the TD-CCSD or TD-CC3 benchmark) is significantly larger than for the other second-order methods TD-CC[2], TD-CC2, and TD-UCC[2]. A formal perturbative analysis given in Paper I shows that the stationary conditions (and consequently the amplitude responses and the corresponding linear-response function which is equivalent to the FDP) differ only in the third order between TD-VCC[2] and TD-CC[2]. Hence, the FDPs obtained using these two second-order methods are indeed expected to be of a similar quality.

However, the similarity of polarizabilities through the second **W** order does not mean automatically that *excitation energies* agree up to the same order, too. In Paper I it was shown that the connection between the TD-CC[2] and TD-VCC[2] stationary conditions involves the $\eta^{Y[\leqslant 2]\dagger}$ term. This term, however, does not enter the Jacobian itself and thus is of no relevance for the eigenvalue problem. As a result the Jacobian matrices of these methods deviate not in the third, as the FDP, but already in the second **W** order. The perturbative analysis of the quality of the excitation energies cannot be directly based on the perturbative analysis of the stationary conditions or quasienergy, since in the vicinity of the poles the **G**-matrix becomes singular, while the amplitudes (parameter responses) become infinite and, thus, cannot be expanded in a perturbative series.

However, what can be analyzed in terms of the perturbative orders with respect to **W** is the completeness of the truncated expressions for the individual elements or blocks of the Jacobian matrix itself, which in turn determines the excitation energies. As was already stated in Paper I, the TD-CC[2], TD-VCC[2], and TD-UCC[2] Jacobians differ in the singles-singles block only. For all three methods, and in particular also for TD-VCC[2], the singles-singles block of the Jacobian contains all possible second-order terms with respect to **W** as dictated by the respective CC *Ansatz* (cf. Sec. IV D in Paper I). In other words, those terms, which are absent in the singles-singles block of the TD-CC[2], TD-VCC[2], and TD-UCC[2] Jacobians, but present there in the respective untruncated methods, are at least of third order with respect to **W**. Nevertheless, and somewhat contradictive at first glance, these three Jacobians deviate from each other in the singles-singles block already in the second order with respect to **W**, as discussed above. These two, seemingly contradictive statements imply that for excited states dominated by single excitations, all three methods are formally correct through the second order with respect to **W** [40,56,78], *but with reference to different untruncated forms of the Jacobian*. Consequently, relatively large deviations in the excitation energies may occur.

Assuming that the three untruncated methods yield all the same excitation energies (though not necessarily from identical Jacobians), one can conclude that the convergence rate of the perturbation expansion of individual elements or blocks of the Jacobian can differ for the three different formalisms. From the numerical experiments presented in Sec. III B, we know that the TD-VCC[2] excitation energies are noticeably smaller (usually by $\sim$0.2 eV, but in some cases by 0.5–0.7 eV) than the TD-UCC[2] and TD-CC2 values, which in turn also underestimate the TD-CCSD benchmark. This suggests that the additional terms in the VCC Jacobian are not beneficiary and do not lead to higher or even similar accuracy compared to TD-CC[2], TD-UCC[2], or TD-CC2. It thus appears that the convergence (with respect to the perturbative order n) is slower for the TD-VCC[n] Jacobian than for the TD-UCC[n] or TD-CCn ones.

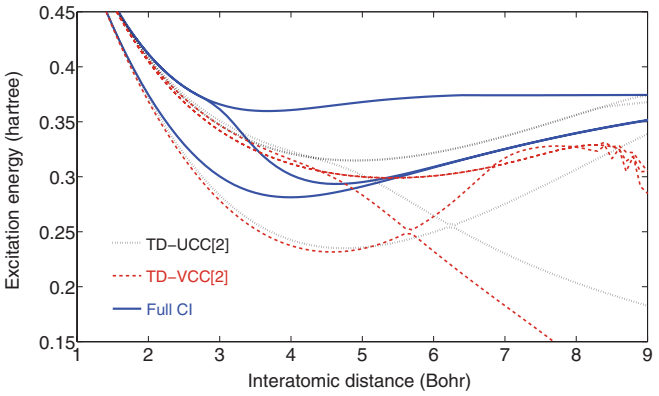

FIG. 1. (Color online) The excitation energies for the H_2 molecule as a function of the distance between the nuclei, calculated using MP2 (ground state), TD-UCC[2], TD-VCC[2], and full CI methods.

In order to test this conjecture we compare the quality of the perturbative expansion (truncated at second order) for the two *Ansätze* VCC and UCC for a system with decreasing quality of the reference wave function. To this end we have plotted in Fig. 1 the TD-VCC[2] and TD-UCC[2] excitation energies for some of the lowest excited states of the H_2 molecule as a function of the internuclear distance R, along with the benchmark curves calculated with TD-CCSD. The latter method is, in contrast to any second-order method, exact for two-electron systems. Furthermore, the second-order methods are expected to deteriorate substantially with increasing multireference character. All calculations employ the aug-cc-pVTZ basis set. In Appendix B, analogous plots of the corresponding ground- and excited-state potential energy surfaces are provided, in addition.

Evidently, for bond lengths close to the ground-state equilibrium the TD-VCC[2] excitation energies lie systematically below those of TD-UCC[2], as already discussed in Sec. III B. Beyond $R = 2.5$ bohrs, i.e., at the onset where the ground state starts to acquire multireference character, the excitation energies of both second-order methods start to deviate noticeably from the benchmark. In the range of $R = 4$–6 bohrs the excitation energies of the two second-order methods start to deviate significantly also from each other, with TD-VCC[2] starting to diverge earlier. Furthermore, in the range of $R = 8$–9 bohrs the behavior of TD-VCC[2] becomes catastrophic, whereas the TD-UCC[2] excitation energies are of course incorrect, but still stable at these distances. This indicates that with decreasing weight of the reference wave function TD-VCC[2] indeed breaks down earlier than TD-UCC[2].

The instability problem of TD-VCC[2] between $R =$ 8 and 9 bohrs can be traced back to the singularity of the metric matrix **M**, Eq. (23), which is equal to just the identity matrix

for the TD-UCC[2] and TD-CC2 formalisms. For TD-VCC[2], on the other hand, additional terms $\langle 0|\tau_{\mu_1}\mathbf{T}_2^{[1](0)\dagger}\mathbf{T}_2^{[1](0)}\tau_{\mu_1}|0\rangle_C$ contribute to **M**. For the simple case of H_2 in the minimal basis it can directly be shown (by summing up all corresponding diagrams) that these contributions have to be negative. Provided that the reference wave function has a large weight, these negative contributions are much smaller in magnitude than the identity matrix, and the overall **M** matrix remains regular. However, when the weight of the reference wave function becomes very small, the MP2 ground-state doubles amplitudes substantially grow, and, at some point, the corresponding negative contribution to the **M** matrix becomes of the order of 1; hence the overall **M** matrix becomes itself close to singular.

The breakdown of TD-VCC[2] vs TD-UCC[2] for increasing internuclear separation R in the H_2 molecule indeed supports the explanation of a slower convergence of the perturbative expansion of the TD-VCC[n] Jacobian for the worse performance of the TD-VCC[2] method compared to TD-CC[2] or TD-UCC[2] as far as excitation energies are concerned. But what could be the reason for the slower convergence of the perturbative expansion of the TD-VCC Jacobian vs TD-UCC or TD-CC? For the corresponding untruncated methods the amount of terms entering the individual elements or blocks of the respective Jacobian indeed strongly depends on the *Ansatz*: In standard CC theory the BCH commutator series necessarily truncates after the fourfold-nested commutator, whereas in the connected forms of the UCC and VCC theory the series is essentially infinite, i.e., it does not terminate even when the excitation level exhausts the number of electrons (cf. Secs. II B and II C). This implies that in the untruncated TD-VCC and TD-UCC formalisms each element of the Jacobian contains a huge amount of higher-order terms, much more numerous than in the untruncated TD-CC Jacobian based on traditional CC theory. By their sheer amount the overall contribution of all these higher-order terms together might be of lower order than is formally attributed to the individual terms themselves. This obviously can slow down the convergence rate of the perturbative expansion.

Nevertheless, TD-UCC[2] provides excitation energies in close agreement with TD-CC2 and even virtually identical to TD-CC[2], as discussed in Sec. III B. Indeed, the difference between the Jacobians of TD-UCC[2] and TD-CC[2], although of second order as well, is rather minor and only in the off-diagonal elements of the singles-singles block [21], i.e.,

$$\begin{aligned}&\tfrac{1}{2}\langle 0|\tau_{\mu_1}\big(\mathbf{W}\mathbf{T}_2^{[1](0)}+\mathbf{T}_2^{[1](0)\dagger}\mathbf{W}\big)\tau_{\nu_1}|0\rangle\\ &\quad\Leftrightarrow\ \langle 0|\tau_{\mu_1}\mathbf{W}\mathbf{T}_2^{[1](0)}\tau_{\nu_1}|0\rangle.\end{aligned}$$

We note in passing, that this link between the TD-CC[2] and TD-UCC[2] Jacobians through symmetrization of the former is lost at higher orders, and the symmetrized TD-CCSD Jacobian no longer delivers exact results for a two-electron system. In contrast, the TD-VCC[2] Jacobian differs from the other two Jacobians in a more fundamental way: Here the second-order terms

$$\langle 0|\tau_{\mu_1}\mathbf{T}_2^{[1](0)\dagger}\mathbf{F}\mathbf{T}_2^{[1](0)}\tau_{\nu_1}|0\rangle_C \quad\text{and}\quad \langle 0|\tau_{\mu_1}\mathbf{T}_2^{[1](0)\dagger}\mathbf{T}_2^{[1](0)}\tau_{\nu_1}|0\rangle_C,$$

either canceling out or being absent altogether in the other two methods, enter the **A** and **M** matrices [cf. Eqs. (14) and (23), respectively]. Terms of this type appear also in higher orders, but again only in the TD-VCC formalism. The influence of these terms on the excitation energies is more substantial, as numerical experiments conducted in the course of this work clearly showed. Therefore, we conclude that the perturbative expansion of mainly these terms suffers from a slow convergence with respect to perturbative orders in **W**.

Furthermore, the possible singularity of the **M** terms appears to be a feature of the connected, but infinite summation of the VCC formalism, cf. Eq. (18). If the *disconnected* diagrams of type

$$\langle 0|\tau_{\mu_1}\mathbf{T}_2^{[1](0)\dagger}\mathbf{T}_2^{[1](0)}\tau_{\mu_1}|0\rangle_D$$

are added to the **M** matrix, the corresponding diagonal elements become positive, as expected from the metric matrix. The singularity problem then disappears. The initial TD-VCC energy expression Eq. (17) indeed contains all these disconnected terms, as well as the denominator, but is free of EPV terms. Therefore, the series in the VCC expectation value expression terminates at the excitation level which exhausts the number of electrons. From this angle, a VCC approach, starting from Eq. (17) rather than (18), should be free of at least this particular problem of the potential singularity of the **M** matrix. On the other hand, in the untruncated VCC formalism based on the connected form (18), the **M**-matrix instability has to be removed by terms of formally higher orders, which sum up such that they cancel with the problematic lower-order terms. This obviously cannot be fulfilled for VCC formalisms truncated at a certain perturbative order like TD-VCC[2].

IV. CONCLUSIONS

In this contribution we discussed the time-dependent CC linear-response theories for two possible Hermitian second-order CC *Ansätze*. The performance of these two methods, denoted as TD-VCC[2] and TD-UCC[2]-H, respectively, was numerically tested by calculating excitation energies and dynamic dipole polarizabilities for several test systems. Two alternative parametrizations based on the UCC *Ansatz*, denoted as TD-UCC-D and TD-UCC-T, were only analyzed theoretically, but not implemented and numerically tested, since they do not lead to a Hermitian eigenvalue problem for the excitation energies. The working equations for excitation energies and polarizabilities of the TD-UCC[2]-H method turned out to be equivalent to those of the already known algebraic-diagrammatic construction propagator approach of second-order, ADC(2). Comparison with other methods reveals that TD-UCC[2]-H provides reasonably good results for excitation energies and polarizabilities, quite similarly to the TD-CC2 approach, i.e., to response theory based on the traditional CC2 model. The performance of the other Hermitian method, TD-VCC[2], is mixed. It provides dynamic dipole polarizabilities of similar quality as other second-order methods (TD-UCC[2]-H, TD-CC2), but excitation energies are systematically too low by at least 0.2 eV (or even more for some test cases), relative to the other second-order methods, which, in turn, also underestimate the TD-CCSD benchmark themselves. This failure of the TD-VCC[2] method was further analyzed in the present work: The Jacobians of TD-VCC[2] and TD-UCC[2]-H deviate from that of TD-CC[2] already in second order with respect to the fluctuation potential **W**, even

though the relevant singles-singles blocks of these Jacobians include all possible second-order terms as dictated by the respective CC *Ansatz*. The additive separability was checked and compared for the individual methods, but turned out to be unproblematic for all the methods, including TD-VCC[2]. Furthermore, the quality of the second-order description with respect to the fluctuation potential was compared for TD-VCC[2] and TD-UCC[2]-H for the case of a H_2 molecule with increasing distance between the nuclei. It turns out that TD-VCC[2] breaks down earlier than TD-UCC[2]-H. Based on the analysis presented here, we conjecture a slower convergence of the perturbative series in the TD-VCC[n] form of the Jacobian, as an explanation for the failure of TD-VCC[2] for excitation energies. This is intimately connected with the nonterminating series obtained for the expansion of the time-dependent VCC quasienergy in its fully connected form, and with the occurrence of additional diagrams contributing to the metric matrix, which involve ground-state amplitudes.

ACKNOWLEDGMENTS

T.K. acknowledges the support from the National Science Centre of Poland through Grant No. 2011/01/B/ST4/06141. Financial support of the Deutsche Forschungsgemeinschaft DFG (Grants No. Ka 3326/1, US 103/1, and SCHU 1456/9) is gratefully acknowledged.

APPENDIX A: THE TD-UCC METHOD

1. Zeroth- and first-order expressions

For the TD-UCC-H *Ansatz* (33) the expectation value of the UCC quasienergy (35) can be written as a double BCH commutator expansion, with the innermost similarity transformation (which is expanded first) originating from the *time-independent* exponentials, i.e.,

$$
\begin{aligned}
Q^H(t) &= \langle \tilde{\Psi}^H_{\mathrm{UCC}} | \bar{\mathbf{H}}(t) | \tilde{\Psi}^H_{\mathrm{UCC}} \rangle \\
&= \langle 0| \exp\left(\mathbf{T}^{(\geqslant 1)\dagger}(t) - \mathbf{T}^{(\geqslant 1)}(t)\right) \exp(\mathbf{T}^{(0)\dagger} - \mathbf{T}^{(0)}) \bar{\mathbf{H}} \exp\left(\mathbf{T}^{(0)} - \mathbf{T}^{(0)\dagger}\right) \exp(\mathbf{T}^{(\geqslant 1)}(t) - \mathbf{T}^{(\geqslant 1)\dagger}(t)) |0\rangle \\
&= \langle 0| \exp\left(\mathbf{T}^{(\geqslant 1)\dagger}(t) - \mathbf{T}^{(\geqslant 1)}(t)\right) \big(\bar{\mathbf{H}} + [\bar{\mathbf{H}}, \mathbf{T}^{(0)} - \mathbf{T}^{(0)\dagger}] + \tfrac{1}{2}[[\bar{\mathbf{H}}, \mathbf{T}^{(0)} - \mathbf{T}^{(0)\dagger}], \mathbf{T}^{(0)} - \mathbf{T}^{(0)\dagger}] + \cdots \big) \\
&\quad \times \exp\left(\mathbf{T}^{(\geqslant 1)}(t) - \mathbf{T}^{(\geqslant 1)\dagger}(t)\right) |0\rangle \\
&= \langle 0| \bar{\mathbf{H}} + [\bar{\mathbf{H}}, \mathbf{T}^{(\geqslant 1)}(t) - \mathbf{T}^{(\geqslant 1)\dagger}(t)] + \tfrac{1}{2}[[\bar{\mathbf{H}}, \mathbf{T}^{(\geqslant 1)}(t) - \mathbf{T}^{(\geqslant 1)\dagger}(t)], \mathbf{T}^{(\geqslant 1)}(t) - \mathbf{T}^{(\geqslant 1)\dagger}(t)] + \cdots + [\bar{\mathbf{H}}, \mathbf{T}^{(0)} - \mathbf{T}^{(0)\dagger}] \\
&\quad + [\bar{\mathbf{H}}, \mathbf{T}^{(0)} - \mathbf{T}^{(0)\dagger}], \mathbf{T}^{(\geqslant 1)}(t) - \mathbf{T}^{(\geqslant 1)\dagger}(t)] + \tfrac{1}{2}[[[\bar{\mathbf{H}}, \mathbf{T}^{(0)} - \mathbf{T}^{(0)\dagger}], \mathbf{T}^{(\geqslant 1)}(t) - \mathbf{T}^{(\geqslant 1)\dagger}(t)], \mathbf{T}^{(\geqslant 1)}(t) - \mathbf{T}^{(\geqslant 1)\dagger}(t)] + \cdots \\
&\quad + \tfrac{1}{2}[[\bar{\mathbf{H}}, \mathbf{T}^{(0)} - \mathbf{T}^{(0)\dagger}], \mathbf{T}^{(0)} - \mathbf{T}^{(0)\dagger}] + \tfrac{1}{2}[[[\bar{\mathbf{H}}, \mathbf{T}^{(0)} - \mathbf{T}^{(0)\dagger}], \mathbf{T}^{(0)} - \mathbf{T}^{(0)\dagger}], \mathbf{T}^{(\geqslant 1)}(t) - \mathbf{T}^{(\geqslant 1)\dagger}(t)] \\
&\quad + \tfrac{1}{4}[[[[\bar{\mathbf{H}}, \mathbf{T}^{(0)} - \mathbf{T}^{(0)\dagger}], \mathbf{T}^{(0)} - \mathbf{T}^{(0)\dagger}], \mathbf{T}^{(\geqslant 1)}(t) - \mathbf{T}^{(\geqslant 1)\dagger}(t)], \mathbf{T}^{(\geqslant 1)}(t) - \mathbf{T}^{(\geqslant 1)\dagger}(t)] + \cdots |0\rangle. \qquad \text{(A1)}
\end{aligned}
$$

The expression for the TD-UCC-D *Ansatz* (34) is obtained in an analogous way, but here the innermost similarity transformation arises from the time-dependent exponentials. For the TD-UCC-T *Ansatz* (32), on the other hand, there is no *ad hoc* exponential factorization into a time-dependent and a time-independent part, hence there is just one (and more complex) BCH expansion for the corresponding quasienergy.

According to Eq. (28) the commutators can be written as connected terms. This yields, e.g., for the TD-UCC-H *Ansatz* (we drop postfix -H and superscript H for simplicity), the following time-averaged quasienergy of second order with respect to the time-dependent perturbation $\mathbf{V}(t)$ (which is relevant for linear-response theory),

$$
\begin{aligned}
\{^{2n+1}Q^{(2)}\}_T = \sum_k \langle 0| &\big(\mathbf{V}\mathbf{T}^{(1)}_1\big)_C + \big(\mathbf{T}^{(1)\dagger}_1 \mathbf{V}\big)_C + (\mathbf{T}^{(1)\dagger}(\mathbf{F}+\mathbf{W})\mathbf{T}^{(1)})_C + ((\mathbf{T}^{(0)\dagger}\mathbf{V})_C \mathbf{T}^{(1)})_C + (\mathbf{T}^{(1)\dagger}(\mathbf{V}\mathbf{T}^{(0)})_C)_C \\
&+ \frac{1}{2}\{((\mathbf{W}\mathbf{T}^{(1)})_C \mathbf{T}^{(1)})_C + (\mathbf{T}^{(1)\dagger}(\mathbf{T}^{(1)\dagger}\mathbf{W})_C)_C + (((\mathbf{T}^{(0)\dagger}(\mathbf{F}+\mathbf{W}))_C \mathbf{T}^{(1)})_C \mathbf{T}^{(1)})_C + (\mathbf{T}^{(1)\dagger}(\mathbf{T}^{(1)\dagger}((\mathbf{F}+\mathbf{W})\mathbf{T}^{(0)})_C)_C)_C \\
&+ (\mathbf{T}^{(1)\dagger}(\mathbf{W}\mathbf{T}^{(0)})_C \mathbf{T}^{(1)})_C + (\mathbf{T}^{(1)\dagger}(\mathbf{T}^{(0)\dagger}\mathbf{W})_C \mathbf{T}^{(1)})_C + ((\mathbf{T}^{(0)\dagger}(\mathbf{V}\mathbf{T}^{(0)})_C)_C \mathbf{T}^{(1)})_C + (\mathbf{T}^{(1)\dagger}((\mathbf{T}^{(0)\dagger}\mathbf{V})_C \mathbf{T}^{(0)})_C)_C + \cdots\} \\
&- \omega_k (\mathbf{T}^{(1)\dagger}\mathbf{T}^{(1)})_C |0\rangle. \qquad \text{(A2)}
\end{aligned}
$$

The superscript $2n+1$ indicates that the $2n+1$ rule in $\mathbf{V}$ has been utilized. With the above expression at hand it is now straightforwardly possible to derive the working equations for the different orders of TD-UCC[n].

In zeroth order, i.e., TD-UCC[0], the ground-state amplitudes, which are at least of first order with respect to the fluctuation potential $\mathbf{W}$, do not contribute. In this case, all three *Ansätze* TD-UCC[0]-H, TD-UCC[0]-D, and TD-UCC[0]-T yield the same time-averaged quasienergy

$$
\begin{aligned}
\{^{2n+1}Q^{[0](2)}\}_T &= \sum_k \langle 0| \big(\mathbf{V}^{-\omega_k}\mathbf{T}^{[0](1)}_{1(\omega_k)}\big)_C + \big(\mathbf{T}^{[0](1)\dagger}_{1(\omega_k)}\mathbf{V}^{\omega_k}\big)_C + \frac{1}{2}\big\{\big(\mathbf{T}^{[0](1)\dagger}_{1(\omega_k)}\big((\mathbf{F}-\omega_k)\mathbf{T}^{[0](1)}_{1(\omega_k)}\big)_C\big)_C + \big(\big(\mathbf{T}^{[0](1)\dagger}_{1(\omega_k)}(\mathbf{F}-\omega_k)\big)_C \mathbf{T}^{[0](1)}_{1(\omega_k)}\big)_C\big\}|0\rangle \\
&= \sum_k \langle 0| \mathbf{V}^{-\omega_k}\mathbf{T}^{[0](1)}_{1(\omega_k)} + \mathbf{T}^{[0](1)\dagger}_{1(\omega_k)}\mathbf{V}^{\omega_k} + \mathbf{T}^{[0](1)\dagger}_{1(\omega_k)}(\mathbf{F}-\omega_k)\mathbf{T}^{[0](1)}_{1(\omega_k)}|0\rangle_C, \qquad \text{(A3)}
\end{aligned}
$$

which is also equivalent to that of TD-VCC[0]. Applying Eqs. (8) to (A3) yields the quantities

$$\eta^{Y[0]}_{\mu_i} = \langle 0|\mathbf{Y}\tau_{\mu_1}|0\rangle_C, \tag{A4}$$

$$\mathbf{G}^{[0]}_{\mu_i\nu_j}(\omega_Y) = \langle 0|\tau^\dagger_{\mu_1}(\mathbf{F}-\omega_Y)\tau_{\nu_1}|0\rangle_C, \tag{A5}$$

$$\mathbf{B}^{[0]}_{\mu_i\nu_j} = 0, \tag{A6}$$

which specify via Eq. (13) the eigenvalue problem and thus the excitation energies. Obviously, the TD-UCC[0] excitation energies are identical to the HF orbital energy differences, as in the case of TD-VCC[0].

In first order the UCC quasienergies start to differ for the different *Ansätze*. For the TD-UCC[1]-H approach with the time-independent exponential to the left of the time-dependent one (innermost similarity transform is time-independent) the quasienergy reads

$$\begin{aligned}
&\{{}^{2n+1}Q^{[\leqslant 1](2)}_H\}_T \\
&= \sum_k \langle 0|\big(\mathbf{T}^{[\leqslant 1](1)\dagger}_{1(\omega_k)}\mathbf{V}^{\omega_k}\big)_C + \big(\mathbf{V}^{-\omega_k}\mathbf{T}^{[\leqslant 1](1)}_{1(\omega_k)}\big)_C + \Big(\big(\mathbf{T}^{[1](0)\dagger}_2\mathbf{V}^{-\omega_k}\big)_C\mathbf{T}^{[\leqslant 1](1)}_{1(\omega_k)}\Big)_C + \Big(\mathbf{T}^{[\leqslant 1](1)\dagger}_{1(\omega_k)}\big(\mathbf{V}^{\omega_k}\mathbf{T}^{[1](0)}_2\big)_C\Big)_C \\
&\quad + \frac{1}{2}\Big\{\big(\mathbf{T}^{[\leqslant 1](1)\dagger}_{1(-\omega_k)}\big(\mathbf{T}^{[\leqslant 1](1)\dagger}_{1(\omega_k)}\mathbf{W}\big)_C\big)_C + \Big(\big(\mathbf{T}^{[\leqslant 1](1)\dagger}_{1(\omega_k)}(\mathbf{F}+\mathbf{W}-\omega_k)\big)_C\mathbf{T}^{[\leqslant 1](1)}_{1(\omega_k)}\Big)_C + \Big(\mathbf{T}^{[\leqslant 1](1)\dagger}_{1(\omega_k)}\big((\mathbf{F}+\mathbf{W}-\omega_k)\mathbf{T}^{[\leqslant 1](1)}_{1(\omega_k)}\big)_C\Big)_C \\
&\quad + \Big(\big(\mathbf{W}\mathbf{T}^{[\leqslant 1](1)}_{1(-\omega_k)}\big)_C\mathbf{T}^{[\leqslant 1](1)}_{1(\omega_k)}\Big)_C + \Big(\mathbf{T}^{[\leqslant 1](1)\dagger}_{1(-\omega_k)}\big(\mathbf{T}^{[\leqslant 1](1)\dagger}_{1(\omega_k)}\big(\mathbf{F}\mathbf{T}^{[1](0)}_2\big)_C\big)_C\Big)_C + \text{H.c.}\Big\}|0\rangle.
\end{aligned} \tag{A7}$$

Again, the relevant quantities specifying linear-response function (=FDP) and excitation energies are obtained by applying Eqs. (8) to (A7), which yields

$$\eta^{Y[\leqslant 1]H}_{\mu_i} = \langle 0|\big(\mathbf{1}+\mathbf{T}^{[1](0)\dagger}_2\big)\mathbf{Y}\tau_{\mu_1}|0\rangle_C, \tag{A8}$$

$$\mathbf{G}^{[\leqslant 1]H}_{\mu_i\nu_j}(\omega_Y) = \langle 0|\tau^\dagger_{\mu_1}(\mathbf{F}+\mathbf{W}-\omega_Y)\tau_{\nu_1}|0\rangle_C, \tag{A9}$$

$$\mathbf{B}^{[\leqslant 1]H}_{\mu_i\nu_j} = \langle 0|\mathbf{W}\tau_{\mu_1}\tau_{\nu_1} + \mathbf{T}^{[1](0)\dagger}_2\mathbf{F}\tau_{\mu_1}\tau_{\nu_1}|0\rangle_C = 0. \tag{A10}$$

The TD-UCC[1]-H eigenvalue problem hence is equivalent to the CIS eigenvalue problem, since the $\mathbf{B}$ part of the Casida equation cancels for converged $\mathbf{T}^{[1](0)}_2$ amplitudes. The same holds true for TD-VCC[1], as shown in Paper I, as well as ADC(1) [52]. The equivalence between TD-UCC[1]-H, TD-VCC[1], and ADC(1) (but not CIS) is valid also for the η term and thus for the FDPs.

Next, we examine the TD-UCC[1]-D approach with the time-dependent exponential to the left of the time-independent one (innermost similarity transform is time dependent). Here, we obtain for the time-averaged quasienergy

$$\begin{aligned}
\{{}^{2n+1}Q^{[\leqslant 1](2)}_D\}_T &= \sum_k \langle 0|\big(\mathbf{T}^{[\leqslant 1](1)\dagger}_{1(\omega_k)}\mathbf{V}^{\omega_k}\big)_C + \big(\mathbf{V}^{-\omega_k}\mathbf{T}^{[\leqslant 1](1)}_{1(\omega_k)}\big)_C + \frac{1}{2}\Big\{\big(\mathbf{T}^{[\leqslant 1](1)\dagger}_{1(-\omega_k)}\big(\mathbf{T}^{[\leqslant 1](1)\dagger}_{1(\omega_k)}\mathbf{W}\big)_C\big)_C \\
&\quad + \Big(\big(\mathbf{T}^{[\leqslant 1](1)\dagger}_{1(\omega_k)}(\mathbf{F}+\mathbf{W}-\omega_k)\big)_C\mathbf{T}^{[\leqslant 1](1)}_{1(\omega_k)}\Big)_C + \Big(\mathbf{T}^{[\leqslant 1](1)\dagger}_{1(\omega_k)}\big((\mathbf{F}+\mathbf{W}-\omega_k)\mathbf{T}^{[\leqslant 1](1)}_{1(\omega_k)}\big)_C\Big)_C + \Big(\big(\mathbf{W}\mathbf{T}^{[\leqslant 1](1)}_{1(-\omega_k)}\big)_C\mathbf{T}^{[\leqslant 1](1)}_{1(\omega_k)}\Big)_C\Big\}|0\rangle,
\end{aligned} \tag{A11}$$

yielding

$$\eta^{Y[\leqslant 1]D}_{\mu_i} = \langle 0|\mathbf{Y}\tau_{\mu_1}|0\rangle_C, \tag{A12}$$

$$\mathbf{G}^{[\leqslant 1]D}_{\mu_i\nu_j}(\omega_Y) = \langle 0|\tau^\dagger_{\mu_1}(\mathbf{F}+\mathbf{W}-\omega_Y)\tau_{\nu_1}|0\rangle_C, \tag{A13}$$

$$\mathbf{B}^{[\leqslant 1]D}_{\mu_i\nu_j} = \langle 0|\mathbf{W}\tau_{\mu_1}\tau_{\nu_1}|0\rangle_C. \tag{A14}$$

Apparently, the expressions for excitation energies and FDP are equivalent to those of TD-HF. Interestingly, the quasienergy does not contain any time-independent ground-state amplitudes, not even for the FDPs. Unfortunately the resulting eigenvalue equations are not Hermitian, therefore the TD-UCC-D *Ansatz* is not so attractive in the present context, although due to the absence of higher-order ground-state amplitudes in the η-term, it may allow for savings in the calculations of FDPs, compared to the TD-UCC-H (=ADC) method.

Finally, for the TD-UCC[1]-T approach with no *ad hoc* factorization of the exponential into a time-dependent and a time-independent part, the time-averaged quasienergy takes the form

$$\begin{aligned}
\{{}^{2n+1}Q^{[\leqslant 1](2)}_T\}_T &= \sum_k \langle 0|\big(\mathbf{T}^{[\leqslant 1](1)\dagger}_{1(\omega_k)}\mathbf{V}^{\omega_k}\big)_C + \big(\mathbf{V}^{-\omega_k}\mathbf{T}^{[\leqslant 1](1)}_{1(\omega_k)}\big)_C + \frac{1}{2}\Big\{\Big(\big(\mathbf{T}^{[1](0)\dagger}_2\mathbf{V}^{-\omega_k}\big)_C\mathbf{T}^{[\leqslant 1](1)}_{1(\omega_k)}\Big)_C + \Big(\mathbf{T}^{[\leqslant 1](1)\dagger}_{1(\omega_k)}\big(\mathbf{V}^{\omega_k}\mathbf{T}^{[1](0)}_2\big)_C\Big)_C \\
&\quad + \big(\mathbf{T}^{[\leqslant 1](1)\dagger}_{1(-\omega_k)}\big(\mathbf{T}^{[\leqslant 1](1)\dagger}_{1(\omega_k)}\mathbf{W}\big)_C\big)_C + \Big(\big(\mathbf{T}^{[\leqslant 1](1)\dagger}_{1(\omega_k)}(\mathbf{F}+\mathbf{W}-\omega_k)\big)_C\mathbf{T}^{[\leqslant 1](1)}_{1(\omega_k)}\Big)_C + \Big(\mathbf{T}^{[\leqslant 1](1)\dagger}_{1(\omega_k)}\big((\mathbf{F}+\mathbf{W}-\omega_k)\mathbf{T}^{[\leqslant 1](1)}_{1(\omega_k)}\big)_C\Big)_C \\
&\quad + \Big(\big(\mathbf{W}\mathbf{T}^{[\leqslant 1](1)}_{1(-\omega_k)}\big)_C\mathbf{T}^{[\leqslant 1](1)}_{1(\omega_k)}\Big)_C\Big\} + \frac{1}{6}\Big\{\Big(\mathbf{T}^{[\leqslant 1](1)\dagger}_{1(-\omega_k)}\big(\big(\mathbf{T}^{[\leqslant 1](1)\dagger}_{1(\omega_k)}\mathbf{F}\big)_C\mathbf{T}^{[1](0)}_2\big)_C\Big)_C + \Big(\mathbf{T}^{[\leqslant 1](1)\dagger}_{1(-\omega_k)}\big(\mathbf{T}^{[\leqslant 1](1)\dagger}_{1(\omega_k)}\big(\mathbf{F}\mathbf{T}^{[1](0)}_2\big)_C\big)_C\Big)_C \\
&\quad + \text{H.c.}\Big\}|0\rangle,
\end{aligned} \tag{A15}$$

and we obtain by virtue of Eq. (8),

$$\eta^{Y[\leqslant 1]T}_{\mu_i} = \langle 0|\big(\mathbf{1} + \tfrac{1}{2}\mathbf{T}_2^{[1](0)\dagger}\big)\mathbf{Y}\tau_{\mu_1}|0\rangle_C, \tag{A16}$$

$$\mathbf{G}^{[\leqslant 1]T}_{\mu_i\nu_j}(\omega_Y) = \langle 0|\tau^\dagger_{\mu_1}(\mathbf{F}+\mathbf{W}-\omega_Y)\tau_{\nu_1}|0\rangle_C, \tag{A17}$$

$$\mathbf{B}^{[\leqslant 1]T}_{\mu_i\nu_j} = \langle 0|\mathbf{W}\tau_{\mu_1}\tau_{\nu_1} + \tfrac{1}{2}\mathbf{T}_2^{[1](0)\dagger}\mathbf{F}\tau_{\mu_1}\tau_{\nu_1}|0\rangle_C = \tfrac{1}{2}\langle 0|\mathbf{W}\tau_{\mu_1}\tau_{\nu_1}|0\rangle_C. \tag{A18}$$

The resulting η^Y, $\mathbf{G}$, and $\mathbf{B}$ terms correspond to the mean between those of the TD-UCC[1]-H and TD-UCC[1]-D formalisms. For the excitation energies this translates to Casida equations with the $\mathbf{A}$ block identical to CIS or TD-HF, but with the $\mathbf{B}$ block being that of TD-HF times a factor of $1/2$.

2. M-matrix in TD-UCC-H Ansatz

In the following it is shown that for the TD-UCC-H *Ansatz* the metric matrix $\mathbf{M}$ is identical to an identity matrix. To this end, the pure time-derivative part of the TD-UCC-H quasienergy,

$$\begin{aligned}\big\langle\tilde\Psi^H_{\mathrm{UCC}}\big|i\frac{\partial}{\partial t}\big|\tilde\Psi^H_{\mathrm{UCC}}\big\rangle &= \langle 0|\exp(-\mathbf{T}^{(\geqslant 1)}+\mathbf{T}^{(\geqslant 1)\dagger})\exp(-\mathbf{T}^{(0)}+\mathbf{T}^{(0)\dagger})i\frac{\partial}{\partial t}\exp(\mathbf{T}^{(0)}-\mathbf{T}^{(0)\dagger})\exp(\mathbf{T}^{(\geqslant 1)}-\mathbf{T}^{(\geqslant 1)\dagger})|0\rangle\\ &= \langle 0|\exp(-\mathbf{T}^{(\geqslant 1)}+\mathbf{T}^{(\geqslant 1)\dagger})\,i\frac{\partial}{\partial t}\exp(\mathbf{T}^{(\geqslant 1)}-\mathbf{T}^{(\geqslant 1)\dagger})|0\rangle,\end{aligned} \tag{A19}$$

from which the $\mathbf{M}$ terms originate [14,40], is analyzed. In the second equality in the above equation we utilize the fact that any commutator of the inner (time-independent) BCH expansion vanishes, according to Eq. (30). The $\mathbf{M}$ matrix is obtained via Eqs. (6), (8), and (14) from the second-order [with respect to the time-dependent perturbation $\mathbf{V}(t)$] time-averaged quasienergy, or more precisely, from the contribution of the time-derivative part thereof. By carrying out the second (outer) BCH expansion of Eq. (A19) [cf. Eq. (A1)], opening the commutators according to Eq. (30), and taking into account the $2n+1$ rule, the latter is equal to

$$\begin{aligned}\frac{i}{2}\langle 0|\mathbf{T}^{(1)\dagger}\dot{\mathbf{T}}^{(1)} - \dot{\mathbf{T}}^{(1)\dagger}\mathbf{T}^{(1)}|0\rangle_C &= \frac{1}{2}\langle 0|\tau^\dagger(\omega_1 t^{(1)\dagger}(-\omega_{-1})e^{-i\omega_{-1}t}t^{(1)}(\omega_1)e^{-i\omega_1 t} + \omega_{-1}t^{(1)\dagger}(-\omega_1)e^{-i\omega_1 t}t^{(1)}(\omega_{-1})e^{-i\omega_{-1}t}\\ &\quad - \omega_{-1}t^{(1)\dagger}(-\omega_{-1})e^{-i\omega_{-1}t}t^{(1)}(\omega_1)e^{-i\omega_1 t} - \omega_1 t^{(1)\dagger}(-\omega_1)e^{-i\omega_1 t}t^{(1)}(\omega_{-1})e^{-i\omega_{-1}t})\tau|0\rangle_C\\ &= \sum_{k=-N}^{N}\omega_k\langle 0|\tau^\dagger(t^{(1)\dagger}(\omega_k)e^{i\omega_k t}t^{(1)}(\omega_k)e^{-i\omega_k t})\tau|0\rangle_C = \sum_k \omega_k\langle 0|\mathbf{T}^{(1)\dagger}_{(\omega_k)}\mathbf{T}^{(1)}_{(\omega_k)}|0\rangle_C.\end{aligned} \tag{A20}$$

In the first equality of this equation, the cluster operators are written out explicitly according to Eqs. (16) and (9), and in Eq. (9) N is set to $N=1$ for simplicity (cf. discussion at the beginning of Sec. II A). Note that $\omega_{-1} = -\omega_1$. The terms where both frequency-dependent amplitudes correspond to opposite frequencies, are usually eliminated by the time averaging in the later step. Here, however, they appear to be identical apart from an opposite sign and thus cancel already in Eq. (A20), leading to time-independent expression already at that stage. The last expression in Eq. (A20) indicates that, according to Eqs. (8) and (14), the $\mathbf{M}$ matrix of TD-UCC[n]-H linear response theory is identical to the identity matrix for any $\mathbf{W}$-order n.

3. Simplifications in TD-UCC[2]-H

By deriving Eqs. (37) and (A2) in Appendix A1, we have used the simplification,

$$\begin{aligned}&\sum_k\langle 0|\Big[\Big[\Big[\frac{1}{4}[\mathbf{F},\mathbf{T}_2^{[1](0)}-\mathbf{T}_2^{[1](0)\dagger}]+\frac{1}{2}\mathbf{W},\mathbf{T}_2^{[1](0)}-\mathbf{T}_2^{[1](0)\dagger}\Big],\mathbf{T}^{[\leqslant 2](1)}_{1(\omega_k)}-\mathbf{T}^{[\leqslant 2](1)\dagger}_{1(-\omega_k)}\Big],\mathbf{T}^{[\leqslant 2](1)}_{1(-\omega_k)}-\mathbf{T}^{[\leqslant 2](1)\dagger}_{1(\omega_k)}\Big]|0\rangle\\ &= \sum_k\frac{1}{2}\langle 0|\Big[\Big[\Big(\Big(\frac{1}{2}(\mathbf{T}_2^{[1](0)\dagger}\mathbf{F})_C+\mathbf{W}\Big)\mathbf{T}_2^{[1](0)}\Big)_C+\Big(\mathbf{T}_2^{[1](0)\dagger}\Big(\frac{1}{2}(\mathbf{F}\mathbf{T}_2^{[1](0)})_C+\mathbf{W}\Big)\Big)_C,\mathbf{T}^{[\leqslant 2](1)}_{1(\omega_k)}-\mathbf{T}^{[\leqslant 2](1)\dagger}_{1(-\omega_k)}\Big],\\ &\quad \mathbf{T}^{[\leqslant 2](1)}_{1(-\omega_k)}-\mathbf{T}^{[\leqslant 2](1)\dagger}_{1(\omega_k)}\Big]|0\rangle\\ &= \sum_k\frac{1}{2}\langle 0|\mathbf{T}^{[\leqslant 2](1)\dagger}_{1(\omega_k)}\big((\mathbf{W}\mathbf{T}_2^{[1](0)})_C+(\mathbf{T}_2^{[1](0)\dagger}\mathbf{W})_C\big)\mathbf{T}^{[\leqslant 2](1)}_{1(\omega_k)}+\mathbf{T}^{[\leqslant 2](1)\dagger}_{1(-\omega_k)}\mathbf{T}^{[\leqslant 2](1)\dagger}_{1(\omega_k)}(\mathbf{W}\mathbf{T}_2^{[1](0)})_C+(\mathbf{T}_2^{[1](0)\dagger}\mathbf{W})_C\mathbf{T}^{[\leqslant 2](1)}_{1(-\omega_k)}\mathbf{T}^{[\leqslant 2](1)}_{1(\omega_k)}|0\rangle_C,\end{aligned} \tag{A21}$$

which is obtained by repeated application of Eq. (28). Furthermore, in the last equality, after opening all nested commutators, we have utilized the MP2 equations to eliminate all terms containing the Fock operator.

TABLE IV. Dipole polarizabilities of water, formamide, and aniline (all values in a.u.).

Method	α_{xx}		α_{yy}		α_{zz}		α_{yz}[a] or α_{xz}[b]	
Frequency	0.0	0.1	0.0	0.1	0.0	0.1	0.0	0.1
Molecule				Water				
TD-HF	7.726	8.097	9.175	9.399	8.422	8.762		
TD-VCC[2]	9.587	10.163	10.471	10.772	10.076	10.464		
TD-UCC[2]	9.475	10.013	10.383	10.674	9.976	10.346		
TD-CC2	9.789	10.358	10.505	10.800	10.055	10.428		
TD-CCSD	9.078	9.530	9.969	10.232	9.451	9.769		
XCCSD	9.256	9.721	10.142	10.410	9.640	9.966		
XCC2	9.167	9.671	10.051	10.329	9.493	9.837		
XCC2A	9.347	9.863	10.394	10.680	9.775	10.129		
CCSD(T)	9.051		9.909		9.403			
CCSD	8.813		9.755		9.209			
TD-VCC[2]*A*	8.954	9.456	10.044	10.326	9.537	9.891		
TD-VCC[2]*B*	9.639	10.218	10.677	10.983	10.131	10.520		
TD-VCC[2]*C*	9.006	9.510	10.248	10.535	9.594	9.949		
Molecule				Formamide				
TD-HF	18.599	19.237	24.694	25.494	31.622	33.322	0.876	0.929
TD-VCC[2]	21.034	21.905	29.209	30.826	41.005	44.629	1.686	1.868
TD-UCC[2]	20.858	21.680	28.865	30.380	39.976	43.142	1.644	1.811
TD-CC2	21.029	21.881	29.459	31.075	39.566	42.562	1.115	1.225
TD-CCSD	20.227	20.986	27.296	28.508	36.530	38.958	0.850	0.868
XCCSD	20.573	21.348	27.893	29.147	37.649	40.182	0.994	1.022
XCC2	20.369	21.171	27.691	29.116	36.162	38.755	0.733	0.797
XCC2A	20.775	21.588	28.595	30.058	37.714	40.437	0.939	1.016
CCSD(T)	20.156		27.269		36.187		0.722	
CCSD	19.801		26.602		35.352		0.778	
TD-VCC[2]*A*	20.549	21.372	27.598	29.018	37.483	40.622	1.282	1.405
TD-VCC[2]*B*	21.186	22.062	29.681	31.318	41.361	45.001	1.528	1.693
TD-VCC[2]*C*	20.702	21.530	28.068	29.507	37.849	41.005	1.139	1.247
Molecule				Aniline				
TD-HF	50.324	52.580	84.289	90.687	97.156	105.482	0.417	0.411
TD-VCC[2]	53.656	56.498	94.366	103.928	114.086	128.881	−0.103	−0.305
TD-UCC[2]	53.262	55.926	92.846	100.973	111.299	123.729	−0.060	−0.221
TD-CC2	52.834	55.505	90.990	98.623	110.155	122.051	0.050	−0.089
TD-CCSD	51.464	53.895	86.947	93.658	103.562	113.595	0.075	−0.033
XCCSD	52.342	54.821	89.188	96.172	106.446	116.901	0.046	−0.068
XCC2	52.168	54.783	89.788	97.496	107.056	118.559	0.235	0.133
XCC2A	53.376	56.035	92.522	100.465	110.287	122.146	0.253	0.146
CCSD(T)	51.074		85.635		102.190		0.069	
CCSD	50.574		84.915		100.937		0.055	
TD-VCC[2]*A*	53.960	56.777	92.485	102.003	109.378	123.310	0.068	−0.089
TD-VCC[2]*B*	53.387	56.223	95.567	105.107	115.976	130.890	0.077	−0.099
TD-VCC[2]*C*	53.688	56.497	93.675	103.170	111.242	125.288	0.243	0.110

[a]For formamide.
[b]For aniline.

APPENDIX B: GROUND- AND EXCITED-STATE POTENTIAL ENERGY CURVES FOR H_2

In addition to the excitation energies, plotted in Fig. 1 as a function of the internuclear distance R of H_2, we also provide the corresponding potential energy curves in Fig. 2. It is seen that the deficiencies in the excitation energies in an intermediate range very well match the errors in the MP2 ground-state energies, which have an opposite sign with respect to the former. This unexpectedly leads to quite a reasonable description of the potential surfaces of the excited states for a significant range of R (even better than that of the ground state) by both the TD-VCC[2] and the TD-UCC[2] methods. How general this trend is, remains to be investigated. Furthermore, the underestimation of the excitation energy by

TD-VCC[2] relative to TD-UCC[2] compensates the error in the ground-state correlation energy of the MP2 method (which is the same reference for both schemes). This results in a smaller deviation of the TD-VCC[2] excited-state energy from the full CI value compared to TD-UCC[2] (at least for R near the ground-state minimum). At the same time, similarly to the excitation energies, the TD-VCC[2] excited-state energy breaks down earlier for increasing R compared to TD-UCC[2], and exhibits an unstable behavior at large R.

APPENDIX C: DYNAMIC DIPOLE POLARIZABILITIES

Table IV compiles, for the three test molecules water, formamide, and aniline, the FDPs for the two frequencies $\omega = 0.0$ a.u. (static) and $\omega = 0.1$ a.u., for a collection of different methods (TD-HF, TD-VCC[2], TD-UCC[2] = ADC(2), TD-CC2, TD-CCSD, XCCSD [34,36], XCC2, and XCC2A [47,79]). Actually, Table IV is a more comprehensive collection of the results of this work than Table II in Sec. III C, the latter being extracted from the former. Orbital-relaxed CCSD(T) and CCSD static polarizabilities were obtained by the finite-field technique. Furthermore, some variants of the TD-VCC[2] method, denoted as TD-VCC[2]x, $x = A,B,C$, were tested.

The TD-HF polarizabilities evidently differ noticeably from the values of the second-order methods, due to the lack of dynamical electron correlation in the TD-HF description, but in some cases are fortuitously close to the high-order results. As already mentioned in Sec. III, the TD-VCC[2], TD-UCC[2], and TD-CC2 methods provide results of a similar quality. The same applies to the TD-CCSD and XCCSD methods. The XCC method [34] results from an alternative derivation of the second-order molecular properties, where one starts from the polarization propagator formula for exact states and replaces exact unperturbed and first-order wave functions by their CC *Ansätze*. Since the same Jacobian is used in XCC for the first-order wave function as in TD-CC, both methods have the same set of poles on the real-valued energy axis.

Test calculations indicate that TD-CCSD usually yields polarizabilities in somewhat closer agreement with the full CI result than XCCSD [36] (a possible theoretical explanation is offered in Ref. [80]). These earlier findings are confirmed by the results compiled in Table IV: The XCCSD polarizabilities are usually 1%–2% larger than the corresponding TD-CCSD values, which in turn, are in very good agreement with (orbital-relaxed) CCSD(T), available for $\omega = 0.0$. Interestingly, orbital-relaxed CCSD polarizabilities deviate in most cases by a larger amount from the CCSD(T) result than the orbital-unrelaxed ones, i.e., TD-CCSD, even though from a formal **W**-order analysis it follows that orbital-relaxed CCSD should be more accurate. This shows that correctness to a formal **W** order does not necessarily determine the overall accuracy of the method.

Table IV also lists the polarizabilities obtained with a new XCC2 method [47,79]. The XCC2 approach utilizes the TD-CC2 Jacobian for obtaining the t^X amplitude responses (so it has the same poles as TD-CC2), but uses a modified η^X [79], what turns out to be a deciding factor for its success to provide improved polarizabilities relative to the TD-CC2 ones. The propagator formula for XCC2 is a simplified XCCSD formula. For the method denoted as XCC2A in Table II, only the zeroth- and first **W**-order terms remain in η^Y, i.e., the terms 1, 3, and 6 of Eq. (22) and CC2 rather than MP2 ground-state doubles amplitudes are employed. The original XCC2 formulation from Ref. [80] additionally neglects the exchange diagram in the third term of Eq. (22).

Since the examples of XCC2 and XCC2A show that the removal of second-order terms from η^X (in particular, $\mathbf{T}_1$ terms), is beneficial for balancing the quality of approximate polarizabilities, we tested three modified η^X vectors also for the TD-VCC[2] case. The removal of the $\mathbf{T}_1^{[2](0)}$-containing terms from η^X [cf. Eq. (22)] leads to the TD-VCC[2]A method; the neglect of $\mathbf{T}_2^{[2](0)}$-containing terms instead leads to TD-VCC[2]B; finally, the simultaneous omission of both types of terms yields the TD-VCC[2]C method. Note that the possibility to neglect $\mathbf{T}_2^{[2](0)}$ amplitudes is beneficial from the computational point of view, since its evaluation scales as $\mathcal{O}(\mathcal{N}^6)$ with molecular size $\mathcal{N}$, while all other steps of a TD-VCC[2] calculation scale at most as $\mathcal{O}(\mathcal{N}^5)$.

As is evident from Table IV, the omission of the $\mathbf{T}_1^{[2](0)}$-containing terms indeed improves the quality of the polarizabilities with respect to the TD-CCSD benchmark. TD-VCC[2]A and C values obviously are much closer to the TD-CCSD benchmark than the original TD-VCC[2] or TD-CC2 values. Furthermore, the effect of $\mathbf{T}_2^{[2](0)}$-containing terms is small, such that these rather expensive contributions can safely be neglected. The TD-VCC[2]C polarizabilities feature a much better agreement with the TD-CCSD benchmark than TD-VCC[2] itself for the cases of water and formamide, while for aniline the deviation from TD-VCC[2] goes in the right direction, but is not large enough. A similar behavior for molecules with aromatic rings has been found before for XCC2 on a larger test set of molecules [47].

We conclude that stripping η^X from all terms second order with respect to **W** leads to systematically better polarizabilities compared to those of the original TD-VCC[2] method. Yet this cannot be explained by a simple **W**-order analysis and is rather the result of some error cancellation.

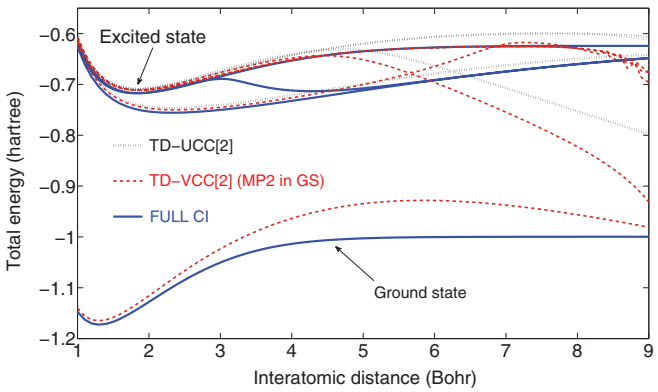

FIG. 2. (Color online) The ground- and excited-state dissociation potential curves for the H_2 molecule calculated using MP2 (ground state), TD-UCC[2] [=ADC(2)], TD-VCC[2], and full CI methods.

[1] J. Cizek, J. Chem. Phys. **45**, 4256 (1966).
[2] R. J. Bartlett and M. Musial, Rev. Mod. Phys. **79**, 291 (2007).
[3] W. Kutzelnigg, Theor. Chim. Acta **80**, 349 (1991).
[4] K. Raghavachari, G. W. Trucks, J. A. Pople, and M. Head-Gordon, Chem. Phys. Lett. **157**, 479 (1989).
[5] C. Hampel and H.-J. Werner, J. Chem. Phys. **104**, 6286 (1996).
[6] M. Schütz, J. Chem. Phys. **113**, 9986 (2000).
[7] M. Schütz and H.-J. Werner, J. Chem. Phys. **114**, 661 (2001).
[8] M. Schütz, J. Chem. Phys. **113**, 8772 (2002).
[9] H.-J. Werner and M. Schütz, J. Chem. Phys. **135**, 144116 (2011).
[10] J. Yang, G. K. L. Chan, F. R. Manby, M. Schütz, and H.-J. Werner, J. Chem. Phys. **136**, 144105 (2012).
[11] T. Helgaker and P. Jørgensen, Adv. Quantum Chem. **19**, 183 (1988).
[12] H. Koch and P. Jørgensen, J. Chem. Phys. **93**, 3333 (1990).
[13] T. B. Pedersen and H. Koch, J. Chem. Phys. **106**, 8059 (1997).
[14] O. Christiansen, P. Jørgensen, and C. Hättig, Int. J. Quantum Chem. **68**, 1 (1998).
[15] J. Geertsen, M. Rittby, and R. J. Bartlett, Chem. Phys. Lett. **164**, 57 (1989).
[16] J. F. Stanton and R. J. Bartlett, J. Chem. Phys. **98**, 7029 (1993).
[17] D. C. Comeau and R. J. Bartlett, Chem. Phys. Lett. **207**, 414 (1993).
[18] H. J. Monkhorst, Int. J. Quantum Chem., Quantum Chem. Symp. **11**, 421 (1977).
[19] D. Mukherjee and P. K. Mukherjee, Chem. Phys. **39**, 325 (1979).
[20] K. Emrich, Nucl. Phys. A **351**, 379 (1981).
[21] C. Hättig, in *Response Theory and Molecular Properties, A Tribute to Jan Linderberg and Poul Jørgensen*, edited by J. Sabin and E. Brändas, Advances in Quantum Chemistry, Vol. 50 (Academic Press, New York, 2005), p. 37.
[22] A. Köhn and A. Tajti, J. Chem. Phys. **127**, 044105 (2007).
[23] P. G. Szalay, M. Nooijen, and R. J. Bartlett, J. Chem. Phys. **103**, 281 (1995).
[24] S. Pal, M. D. Prasad, and D. Mukherjee, Pramana **18**, 261 (1982).
[25] W. Kutzelnigg, in *Recent Progress in Coupled Cluster Methods*, edited by P. Čársky, J. Paldus, J. Pittner, and J. Leszczynski, Challenges and Advances in Computational Chemistry and Physics, Vol. 11 (Springer-Verlag, Berlin, 2010), p. 299.
[26] W. Kutzelnigg, in *Methods of Electronic Structure Theory*, edited by H. F. Schaefer III, Modern Theoretical Chemistry, Vol. 3 (Plenum Press, New York, 1977), p. 129.
[27] R. J. Bartlett, S. A. Kucharski, and J. Noga, Chem. Phys. Lett. **155**, 133 (1989).
[28] A. G. Taube and R. J. Bartlett, Int. J. Quantum Chem. **106**, 3393 (2006).
[29] R. J. Bartlett and J. Noga, Chem. Phys. Lett. **150**, 29 (1988).
[30] B. Jeziorski and R. Moszynski, Int. J. Quantum Chem. **48**, 161 (1993).
[31] J. S. Arponen, Ann. Phys. (NY) **151**, 311 (1983).
[32] J. S. Arponen, R. F. Bishop, and E. Pajanne, Phys. Rev. A **36**, 2519 (1987).
[33] B. Cooper and P. J. Knowles, J. Chem. Phys. **133**, 234102 (2010).
[34] R. Moszynski, P. S. Żuchowski, and B. Jeziorski, Coll. Czech. Chem. Commun. **70**, 1109 (2005).
[35] T. Korona and B. Jeziorski, J. Chem. Phys. **125**, 184109 (2006).
[36] T. Korona, M. Przybytek, and B. Jeziorski, Mol. Phys. **104**, 2303 (2006).
[37] N. Vaval, K. B. Ghose, and S. Pal, J. Chem. Phys. **101**, 4914 (1994).
[38] N. Vaval and S. Pal, Chem. Phys. Lett. **398**, 194 (2004).
[39] J. B. Robinson and P. J. Knowles, J. Chem. Phys. **137**, 054301 (2012).
[40] D. Kats, D. Usvyat, and M. Schütz, Phys. Rev. A **83**, 062503 (2011).
[41] O. Christiansen, P. Jørgensen, and C. Hättig, Int. J. Quantum Chem. **68**, 1 (1998).
[42] H. Koch, H. J. A. Jensen, P. Jørgensen, and T. Helgaker, J. Chem. Phys. **93**, 3345 (1990).
[43] R. J. Wheatley, J. Comput. Chem. **29**, 445 (2008).
[44] P. B. Rozyczko, S. A. Perera, M. Nooijen, and R. J. Bartlett, J. Chem. Phys. **107**, 6736 (1997).
[45] C. Hättig, H. Koch, and P. Jørgensen, J. Chem. Phys. **109**, 3293 (1998).
[46] O. Christiansen, H. Koch, and P. Jørgensen, J. Chem. Phys. **103**, 7429 (1995).
[47] T. Korona, Phys. Chem. Chem. Phys. **12**, 14977 (2010).
[48] J. Čížek, Adv. Chem. Phys. **14**, 35 (1969).
[49] P. G. Szalay and R. J. Bartlett, Int. J. Quantum Chem. **44**, 85 (1992).
[50] M. Head-Gordon, R. J. Rico, M. Oumi, and T. J. Lee, Chem. Phys. Lett. **219**, 21 (1994).
[51] A. G. Taube and R. J. Bartlett, Int. J. Quantum Chem. **106**, 3393 (2006).
[52] J. Schirmer, Phys. Rev. A **26**, 2395 (1982).
[53] M. D. Prasad, S. Pal, and D. Mukherjee, Phys. Rev. A **31**, 1287 (1985).
[54] A. B. Trofimov and J. Schirmer, J. Phys. B **28**, 2299 (1995).
[55] D. Mukherjee and W. Kutzelnigg, in *Many-Body Methods in Quantum Chemistry* (Springer, Berlin, 1989), p. 257.
[56] F. Mertins and J. Schirmer, Phys. Rev. A **53**, 2140 (1996).
[57] J. Goldstone and K. Gottfried, Il Nuovo Cimento **13**, 849 (1959).
[58] A. D. McLachlan and M. A. Ball, Rev. Mod. Phys. **36**, 844 (1964).
[59] S. Hirata, M. Head-Gordon, and R. J. Bartlett, J. Chem. Phys. **111**, 10774 (1999).
[60] H.-J. Werner, P. J. Knowles, G. Knizia, F. R. Manby, M. Schütz, P. Celani, T. Korona, R. Lindh, A. Mitrushenkov, G. Rauhut *et al.*, MOLPRO, version 2010.2, a package of *ab initio* programs (2010), see http://www.molpro.net.
[61] H.-J. Werner, P. J. Knowles, G. Knizia, F. R. Manby, and M. Schütz, Comput. Mol. Sci. **2**, 242 (2012).
[62] D. Kats, D. Usvyat, and M. Schütz, Phys. Chem. Chem. Phys. **10**, 3430 (2008).
[63] D. Kats and M. Schütz, J. Chem. Phys. **131**, 124117 (2009).
[64] K. Freundorfer, D. Kats, T. Korona, and M. Schütz, J. Chem. Phys. **133**, 244110 (2010).
[65] T. Korona and H.-J. Werner, J. Chem. Phys. **118**, 3006 (2003).
[66] T. Helgaker, H. J. A. Jensen, P. Jørgensen, J. Olsen, K. Ruud, H. Ågren, A. A. Auer, K. L. Bak, V. Bakken, O. Christiansen *et al.*, DALTON, an *ab initio* electronic structure program, Release 2.0 (2005), see http://www.kjemi.uio.no/software/dalton/dalton.html.
[67] T. H. Dunning, Jr., J. Chem. Phys. **53**, 2823 (1970).
[68] G. D. Purvis, R. Shepard, F. B. Brown, and R. J. Bartlett, Int. J. Quantum Chem. **23**, 835 (1983).
[69] L. Meissner, J. Chem. Phys. **108**, 9227 (1998).

[70] P. G. Szalay, T. Watson, A. Perera, V. F. Lotrich, and R. J. Bartlett, J. Phys. Chem. A **116**, 6702 (2012).
[71] H. Larsen, J. Olsen, C. Hättig, and P. Jørgensen, J. Chem. Phys. **111**, 1917 (1999).
[72] T. Helgaker, P. Jørgensen, and J. Olsen, *Molecular Electronic Structure Theory* (Wiley, New York, 2000).
[73] M. Nooijen and R. J. Bartlett, J. Chem. Phys. **107**, 6812 (1997).
[74] J. F. Stanton and J. Gauss, J. Chem. Phys. **111**, 8785 (1999).
[75] M. Musiał and R. J. Bartlett, J. Chem. Phys. **129**, 134105 (2008).
[76] T. Korona Mol. Phys. **110**, 199 (2012).
[77] M. Musiał and R. J. Bartlett, J. Chem. Phys. **134**, 034106 (2011).
[78] O. Christiansen, H. Koch, and P. Jørgensen, J. Chem. Phys. **103**, 7429 (1995).
[79] T. Korona, Phys. Chem. Chem. Phys. (to be published).
[80] T. Korona, Mol. Phys. **108**, 343 (2010).